Physics – Uspekhi **57** (4) 359 – 376 (2014)

100th ANNIVERSARY OF THE BIRTH OF Ya B ZELDOVICH

PACS numbers: 04.70.Bw, 97.60.Jd, **98.54. – h**

Black holes in binary stellar systems and galactic nuclei

A M Cherepashchuk

DOI: 10.3367/UFNe.0184.201404d.0387

Contents

Abstract. In the last 40 years, following pioneering papers by Ya B Zeldovich and E E Salpeter, in which a powerful energy release from nonspherical accretion of matter onto a black hole (BH) was predicted, many observational studies of black holes in the Universe have been carried out. To date, the masses of several dozen stellar-mass black holes ($M_{\rm BH} = (4-20)\,M_\odot$) in X-ray binary systems and of several hundred supermassive black holes ($M_{\rm BH} = (10^6-10^{10})\,M_\odot$) in galactic nuclei have been measured. The estimated radii of these massive and compact objects do not exceed several gravitational radii. For about ten stellar-mass black holes and several dozen supermassive black holes, the values of the dimensionless angular momentum a_* have been estimated, which, in agreement with theoretical predictions, do not exceed the limiting value of $a_* = 0.998$. A new field of astrophysics, so-called black hole demography, which studies the birth and growth of black holes and their evolutionary connection to other objects in the Universe, namely stars, galaxies, etc., is rapidly developing. In addition to supermassive black holes, massive stellar clusters are observed in galactic nuclei, and their evolution is distinct from that of supermassive black holes. The evolutionary relations between supermassive black holes in galactic centers and spheroidal stellar components (bulges) of galaxies, as well as dark-matter galactic haloes are brought out. The launch into Earth's orbit of the space radio interferometer RadioAstron opened up the real possibility of finally proving that numerous discovered massive and highly compact objects with properties very similar to those of black holes make up real black holes in the sense of Albert Einstein's General Relativity. Similar proofs of the existence of black holes in the Universe can be obtained by intercontinental radio interferometry at short wavelengths $\lambda \lesssim 1$ mm (the international program, Event Horizon Telescope).

A M Cherepashchuk Sternberg State Astronomical Institute,
M V Lomonosov Moscow State University,
Universitetskii prosp. 13, 119991 Moscow, Russian Federation
E-mail: cherepashchuk@gmail.com

Received 9 October 2013
Uspekhi Fizicheskikh Nauk **184** (4) 387 – 407 (2014)
DOI: 10.3367/UFNr.0184.201404d.0387
Translated by K A Postnov; edited by A Radzig

1. Introduction

A powerful energy release from accreting black holes was predicted in 1964 in pioneering papers by Ya B Zeldovich [1] and E E Salpeter [2]. Since then, astronomers have carried out many observational studies of these enigmatic objects in the Universe.

Black holes are gradually becoming 'true citizens' alongside classical astrophysical objects — stars, galaxies, etc. Observations suggest that the number of stellar-mass black holes ($M = (8-10)\,M_\odot$) in our Galaxy amounts to at least ten million, or 0.1% of the baryonic mass (stars, gas, and dust). This is a significant amount ($\sim 10^8 M_\odot$), so one can speak of the discovery of a new state of matter in the Galaxy in the form of black holes (the collapsing state of matter, in addition to gaseous, liquid, solid, and plasma states). It has become clear that supermassive black holes with $M = (10^6-10^{10})\,M_\odot$ reside in the centers of most galaxies. In particular, there is a black hole with mass $(4.31 \pm 0.36)\times 10^6 M_\odot$ in the center of our Galaxy. The mass of this black hole is determined with an accuracy of better than 10% from the motion of 28 stars orbiting it in elliptic orbits [3] (see Fig. 1). The properties of these numerous and highly compact objects are very similar to those of the black holes predicted by Einstein's General Relativity (GR). That is why, astronomers nowadays would dub these objects (with some reservations) black holes (and not black hole candidates, as, say, they would have thirty years ago).

Nevertheless, it should be recognized that, strictly speaking, up to now no conclusive proof that these compact objects make up black holes in the GR sense has been found. The point is that the main peculiarity of a black hole shows up in the absence of an observable surface; instead, a black hole is surrounded by an event horizon — a light-like surface in spacetime, at which the time dilation for an infinitely remote observer tends to infinity. Meanwhile, proving the absence of an observable surface for a certain object is much more difficult than proving its presence (as is done, for example,

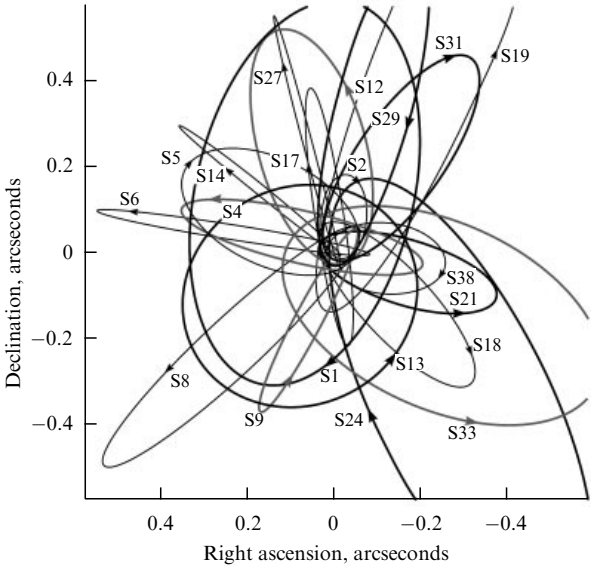

Figure 1. Orbits of stars around the supermassive black hole in the galactic center, which have been used, with the help of the third Kepler law, to determine the black hole mass $M_{\rm BH} = (4.31 \pm 0.36) \times 10^6 M_\odot$ (taken from paper [3]).

in the case of neutron stars which are observed as X-ray pulsars, radio pulsars, or type I X-ray bursters; see, for example, review [4]). It should, however, be stressed that all observational data on numerous black hole candidates (about thirty stellar-mass black holes and many hundreds of supermassive black holes, hereinafter SMBHs) are in excellent agreement with GR predictions for black holes. According to a very precise pronouncement of V L Ginzburg, modern observational data strengthen our belief that black holes really exist in the Universe.

In our review published in *Physics–Uspekhi* in 2003 [4], methods and results of observations of SMBHs and stellar-mass black holes were described in detail. Now, ten years latter, it makes sense to revisit the problem of black holes for the following reasons.

(1) In July 2011, the Russian space radio interferometer RadioAstron was successfully launched into orbit. This unique mission is supervised by Academician N S Kardashev. The radio interferometer allows observations of galactic nuclei with an angular resolution of better than 10^{-5} arcseconds. This opens up the fundamental possibility of investigating processes near event horizons of SMBHs in the nuclei of nearby galaxies and, moreover, of 'seeing' the image of an SMBH, more precisely, the image of the 'dark shadow' formed by the black hole on the bright background of the accretion disk around it. Thus, the real possibility of conclusively proving the existence of black holes in the Universe has appeared.

(2) In 2012, we celebrated the 40th anniversary of the discovery of compact binary X-ray source Cyg X-1, black-hole candidate 'Number One'. As is well known, Prof. Riccardo Giacconi was awarded the Nobel Prize in Physics 2002 "for pioneering contributions to astrophysics, which have led to the discovery of cosmic X-ray sources".

In this review, we describe the present-day observational status of black holes and discuss further prospects for studies of these extreme objects.

2. Exoticism of black holes

We start by recalling the main properties of black holes [5].

Black holes are derived from the collapse (compression) of massive objects. According to modern concepts taking into account GR effects, if the mass of the stellar core where thermonuclear burning occurs exceeds $3M_\odot$, the gravitational core collapse results in the formation of a black hole. If the mass of the stellar core is less than $3M_\odot$, the stellar evolution ends up with the formation of a neutron star or a white dwarf.

A black hole is an object (more precisely, a spacetime region) with so strong a gravitational field that no signal, including light, can escape from it to the space infinity. This means that the parabolic velocity for a black hole is equal to the speed of light $c = 300000$ km s^{-1} in a vacuum. As mentioned above, the event horizon serves as the physical boundary of a black hole. The event horizon makes up a light-like surface in spacetime. An arbitrarily short time interval on the event horizon corresponds to an arbitrarily long time interval in the space infinity. It should be stressed that, for those black holes which are forming at the present time, the event horizon does not have time to form due to relativistic time dilation for the external observer. However, the radius of a collapsing object becomes very close to the event horizon as early as the first seconds of the collapse. For the external observer, all processes on the surface of the collapsing object stretch very strongly in time and become virtually frozen in. Therefore, the surface of such a compact object becomes unobservable. For astronomers, this is 'virtually' the event horizon.

In the center of a black hole, singularity appears with a formally infinite density, where the matter (in the attached reference frame) from which the black hole was formed collapsed. So far unknown physical laws of quantum gravity operate in this singularity; there is no classical space and time any more. However, since the singularity is located in the future with respect to the event horizon, the lack of knowledge about quantum gravity laws does not prevent us from describing the event horizon and the main part of black hole interiors using classical GR. The characteristic size of a black hole is given by the gravitational (Schwarzschild) radius

$$r_{\rm g} = \frac{2GM}{c^2}\,, \tag{1}$$

where M is the mass of the object, G is the Newtonian constant of gravitation, and c is the speed of light in vacuum. The value of the Schwarzschild radius is $r_{\rm g} = 9$ mm for Earth, $r_{\rm g} = 3$ km for the Sun, and $r_{\rm g} = 40$ astronomical units (A.U.) for the object of two billion solar masses (such massive black holes are found in galactic nuclei), which equals the distance between the Sun and the Pluto.

For a nonrotating Schwarzschild black hole, the event horizon radius $r_{\rm h}$ is equal to its gravitational radius: $r_{\rm h} = r_{\rm g}$. For a rotating black hole, the event horizon radius is smaller than the gravitational radius: $r_{\rm h} < r_{\rm g}$. In this case, the event horizon is embedded in an ergosphere which contains the vortex gravitational field. An object having found its way into the ergosphere is caught up by rotating spacetime to begin rotating around the central black hole. It is possible to extract quite a lot of energy from the ergosphere with an efficiency which is much higher than that comprising thermonuclear reactions.

The discontinuities that appear on the event horizon, for example, in the Schwarzschild metric, can be removed by

choosing the appropriate reference frame. For example, no discontinuity at the horizon appears for an observer freely falling into a black hole. Therefore, the freely falling observer can enter the black hole and reach the central singularity, where she or he will be disrupted by enormous tidal forces.

The unique properties of the event horizons of black holes are described in detail in the review by I D Novikov and V P Frolov [6]. The event horizon represents a boundary between different signals propagating with the speed of light. Some of them can escape to the space infinity, some not. Whether a signal can escape the black hole forever depends on a spacetime region located in the future relative to the source of the signal. Therefore, the motion of the black hole event horizon is determined not by its past, but its future (!). This unusual property of the event horizon to 'feel' the future is called by some scientists the 'teleological nature' of the event horizon [6].

In black hole interiors (the so-called T-region [5]), the space and time coordinates interchange from the point of view of the external observer. The structure of spacetime is especially complicated inside a rotating black hole. Here, the so-called Cauchy horizon emerges, which receives information from the formally infinite future of our Universe. Therefore, the structure of spacetime inside a rotating black hole strongly depends on the fate of the black hole itself in the infinite future of the external observer, for example, on possible collisions with other objects, quantum evaporation, and even the future of the entire Universe. As Novikov and Frolov note [6], theoretical physicists are rather uncomfortable with these perplexities...

Indeed, it is difficult to believe in the existence of these really extreme objects. That is why, despite existing enormous observational data on numerous black hole candidates, which is in excellent agreement with GR predictions, scientists try to find crucial evidence of the existence of black holes in the Universe. Moreover, relativistic theories of gravitation alternative to GR have been suggested, which deny the existence of black holes. For example, as was shown in papers by A A Logunov [7] and L P Grishchuk [8], the introduction of a nonzero graviton mass into equations describing gravitational field prevents the formation of event horizons, and a massive collapsing object (more massive than $3M_\odot$) can have an observable surface. This conclusion is radically different from GR predictions, which makes searches for black holes especially intriguing and fascinating.

The final argument in solving this problem should be provided by astronomical observations (we shall not discuss here the hypothetical possibility of the creation of microscopic black holes from elementary particle collisions, which may be realized in Large Hadron Collider experiments in Switzerland).

In the first part of the present review, we summarize the basic observational facts about black holes, and in the second part we discuss prospects for obtaining conclusive proofs that these numerous compact objects are indeed black holes.

3. Stellar-mass black holes in X-ray binary systems

Black holes can be found in X-ray binary systems ($M_{\rm BH} \simeq (4-20)M_\odot$), and in galactic nuclei ($M_{\rm BH} \simeq (10^6-10^{10})\,M_\odot$).

An X-ray binary system consists of a normal optical star like our Sun (the donor of matter) and a relativistic compact object, a neutron star or black hole, which accretes matter from the companion. Tidal attacks of the gravitational field of the relativistic object deform the optical companion and induce matter outflow from it, thus forming an accretion disk around the compact star. Central parts of the disk have a high temperature and mostly emit in the X-ray range. In transient (bursting) X-ray binaries with rapidly rotating massive normal companions of O–B spectral types, accretion onto the relativistic object usually occurs from the equatorial stellar wind launched by rapid axial rotation of the optical star. In the so-called WR + C X-ray binaries, as well as in some symbiotic systems, accretion proceeds from the radially outflowing stellar wind of a Wolf–Rayet (WR) star or a red giant star.

To date, specialized X-ray satellites (UHURU, Einstein, ROSAT (a contraction of German Röntgensatellit), Mir–Kvant, GRANAT, Ginga, Chandra, XMM-Newton (X-ray multi-mirror mission-Newton), INTEGRAL (INTErnational Gamma-Ray Astrophysics Laboratory), etc.) have discovered more than one thousand X-ray binaries, which serve as a powerful tool in the detection and studies of stellar-mass black holes.

As mentioned in the Introduction, Ya B Zeldovich [1] and E E Salpeter [2] showed in 1964 that a nonspherical accretion of matter onto a black hole should be accompanied by a huge energy release due to the emergence of an enormous gravitational potential in the vicinity of black holes. The theory of disk accretion was constructed in 1972–1973 in papers by Shakura and Sunyaev [9], Pringle and Rees [10], and Novikov and Thorne [11]. A more detailed discussion of X-ray binary studies can be found in reviews [4, 12–14] (see also monograph [15]).

The idea to measure black hole masses in binary systems using the mass function of the optical star, which can be obtained by optical Doppler spectroscopy, was first suggested by O Kh Guseinov and Ya B Zeldovich [16].

X-ray and optical observations of X-ray binary systems perfectly complement each other. X-ray observations from space vehicles (Earth's atmosphere is opaque to X-ray quanta) allow one to foresee the presence of a compact star in a binary system, while measurements of rapid X-ray time variability on timescales Δt as short as 10^{-3} s provide an estimate of the characteristic size of a compact star: $r \lesssim c\Delta t$, where c is the speed of light. These estimates imply that the sizes of compact X-ray sources never exceed several gravitational radii. At the same time, spectral and photometric observations by ground-based optical telescopes enable us to study the motion of the normal optical star in an X-ray binary system and to deduce, using the star as a 'test body', the mass of the black hole or neutron star from Newton's law of gravitation. Because the orbital size of an X-ray binary is usually found to be as high as millions of the gravitational radii of its components, the application of a Newton law of gravitation in this case is well justified. This implies that values of black hole masses determined from optical observations of X-ray binaries are independent of the specific relativistic theory of gravity, because all these theories (including alternatives to GR, which deny the existence of black holes) at large distances from the gravitating object are consistent with Newtonian gravity. Note, going ahead, that this conclusion is also valid for masses of SMBHs in galactic nuclei, which were derived from optical observations of the motions of 'test bodies' (stars, gas disks, gas clouds, etc.).

If the measured mass of an X-ray source exceeds $3M_\odot$, it can be considered as a black hole candidate. Just this

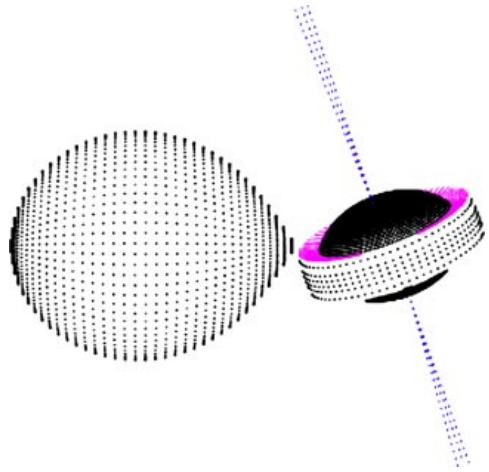

Figure 2. Schematic image based on which a mathematical model of an X-ray binary system with a supercritical accretion disk precessing around the compact central object and collimated relativistic jets is constructed.

determines the strategy of searching for stellar-mass black holes in binary systems.

The first optical identifications of X-ray binary systems and studies of their optical manifestations (ellipticity and reflection effects) were carried out in 1972–1973 and reported in papers [17–20]. Based on these studies, reliable methods of estimating the black hole masses in X-ray binaries were developed (see, for example, books [15, 21]). Methods of interpreting light curves, line profiles, and radial velocity curves of X-ray binaries were devised by assuming that the optical star is not a point-like object but has a finite size, an ellipsoidal or pear-like shape with a complex surface temperature distribution (see Figs 2 and 3). The application of this realistic model of X-ray binaries in combination with modern mathematical methods of solving inverse parametric problems in the statistical formulation allows us to compare the simulated results with observations, to evaluate the parameters of X-ray binaries, and to estimate their errors.

To date, some scientific groups (from the USA, the UK, Germany, the Netherlands, France, Russia, and some other countries) have measured the masses of 26 stellar-mass black holes ($M_{\rm BH} \simeq (4-20)\,M_\odot$), as well as the masses of more than 50 neutron stars ($M_{\rm NS} \simeq (1-2)\,M_\odot$) in binary systems (see Fig. 4).

The masses of 26 black holes in X-ray binaries are listed in Table 1, including values which need to be improved in future observations. The reliability of determining the black hole mass is further discussed in monograph [15], where references to the original papers on individual black hole mass estimations can also be found.

The measured masses of neutron stars lie within the range of $(1-2)\,M_\odot$, with the mean neutron star mass being $\sim 1.4M_\odot$. Fine differences in various types of neutron stars have already been found. For example, the masses of rapidly rotating old neutron stars (spin periods of about one ms), which have been recycled by accretion in close binary systems [22], are on average $\sim 0.15M_\odot$ higher than the masses of slowly rotating neutron stars (spin periods of about several ms) [23]. This inference is consistent with theoretical predictions [24]. All neutron stars with measured masses demonstrate clear signatures of their surfaces — they are either radio pulsars, X-ray pulsars, or type I X-ray bursters.

Let us recall that the X-ray pulsar phenomenon reflects the presence of hot X-ray regions (shocks) near the magnetic

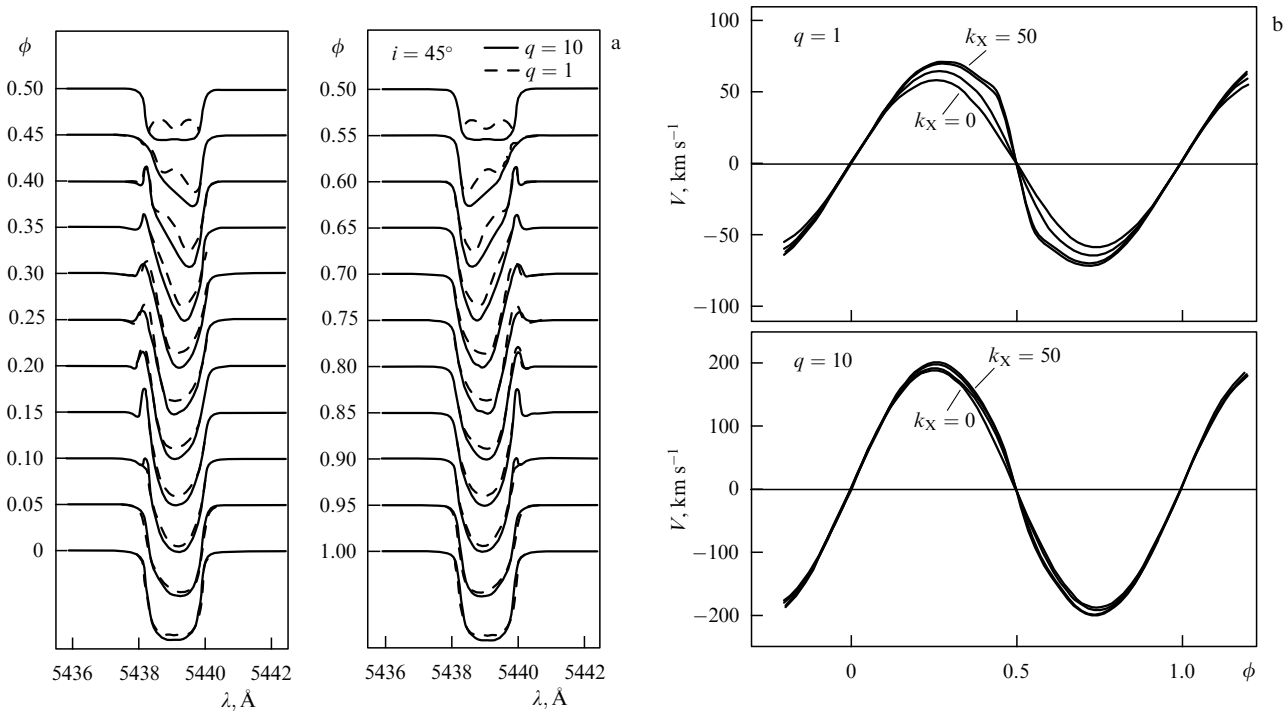

Figure 3. (a) Changes in Ca I absorption line profile in the optical spectrum of an X-ray binary system with an orbital period phase which are caused by tidal deformation of the star and heating of its surface by X-ray emission from accreting compact object. For convenience of profile comparison, Doppler shifts of lines due to orbital revolution are removed: ϕ is the orbital period phase, i is the binary orbit inclination (the angle between the binary orbital plane and the sky plane). (b) The corresponding radial velocity curves for different values of the component mass ratio q and for different values of the X-ray heating parameter k_X. The binary orbit is circular.

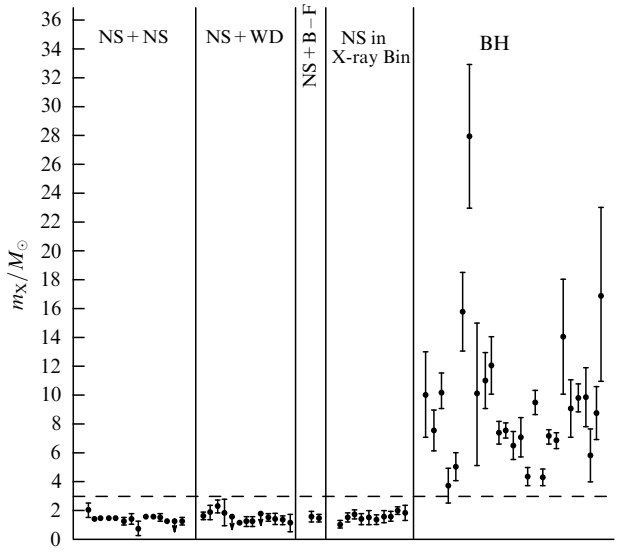

Figure 4. Measured masses of neutron stars (NS) and black holes (BH) in binary stellar systems: NS + NS — binary radio pulsars with neutron stars, NS + WD — binary radio pulsars with white dwarfs, NS + B-F — binary radio pulsars with an optical nondegenerate star of the B-F spectral class, and NS in X-ray Bin — binary X-ray pulsars. The dashed horizontal line shuts off the value of $3M_\odot$ — the absolute upper limit of neutron star masses predicted by GR.

poles of rapidly rotating, strongly magnetized, accreting neutron stars. The radio pulsar phenomenon is due to the rapid rotation of a neutron star and its strong magnetic field, which is 'tied' to its surface. The type I X-ray burster appears due to thermonuclear explosions of matter collected on the surface of an accreting neutron star with a weak magnetic field. Clearly, all three phenomena would be impossible if neutron stars had no observable surfaces. It should be emphasized that rapid rotation and the strong magnetic field of a neutron star are the natural consequences of the strong contraction of a star to very small sizes of order 10 km. Thus, in all cases where a compact star demonstrates clear signatures of an observable surface, its measured mass ranges $(1-2)M_\odot$ and does not exceed $3M_\odot$, in full agreement with the GR prediction of the existence of an upper mass limit for neutron stars (!). We recall that the number of measured neutron star masses is already higher than fifty, so the statistics in this case are quite reliable.

Consider now the observed properties of black hole candidates (see Table 1). The measured masses of 26 candidates fall within the range $(4-20)\,M_\odot$, with the mean mass being of order $9M_\odot$. As black holes have no observable surface, they should not show up as a radio pulsar, X-ray pulsar, or type I X-ray burster. This is indeed the case for 26 black hole candidates listed in Table 1: none (!) of these massive ($M > 3M_\odot$), compact (radii do not exceed a few r_g) X-ray sources has shown evidence of a radio pulsar, X-ray pulsar, or type I X-ray burster. All of them demonstrate only irregular or quasiperiodic (but not strictly periodic) X-ray emission variability down to timescales as short as $\sim 10^{-3}$ s. In the model which takes into account oscillations of the inner parts of the accretion disk or the orbital motion of hot spots in the inner parts of the disk, it is possible to show [25] that such a rapid X-ray variability of black hole candidates is due to their very small sizes not exceeding several gravitational radii.

Notice that, in addition to the distinct observational manifestations of neutron stars and black hole candidates described above, there are more sophisticated differences which are related to the shape and time characteristics of their X-ray spectra (see, for example, Ref. [26]). These fine differences also suggest that neutron stars possess observable surfaces, while black hole candidates do not (!).

Thus, a remarkable result gradually emerges with the increasing bulk of information on the masses of relativistic compact stars: neutron stars and black hole candidates differ not only in masses, but also in other observational manifestations, in full quantitative agreement with GR. Near the theoretical upper limit $3M_\odot$ of neutron star masses (the absolute mass limit for a neutron star in GR), there appears a gap in observational manifestations of relativistic compact stars. In agreement with GR, those with masses of more than $3M_\odot$ do not show signatures of the presence of observable surfaces, and in the cases where such signatures are found, the masses of the objects always turn out to be less than $3M_\odot$.

Therefore, all necessary conditions imposed by GR on the observational appearance of accreting black holes are satisfied. Unfortunately, so far we do not have sufficient criteria for selecting true black holes from the detected candidates. The point is that some neutron stars, like black holes, can show no signatures of the observable surface. For example, the X-ray pulsar phenomenon does not occur if the dipole magnetic field is aligned with the neutron star spin axis. Should this be the case, it is possible to mistake a heavy neutron star for a black hole. Therefore, taking into account the almost fantastic properties of black holes described above, we should conclude with caution that if GR is true in extremely strong gravitational fields, black holes have undoubtedly been discovered. But if we want to check GR in extremely strong gravitational fields, we should prove by direct observations that black holes do not have observable surfaces, but have event horizons and ergospheres.

In this connection, the author of the present review has sometimes been reproached for being excessively cautious and conservative. However, the experience in applications of GR to describing the Universe on large scales seems to justify such cautiousness. Indeed, we had been sure until 1998 that GR without the Λ-term correctly describes the large-scale structure and dynamics of the Universe. However, an unexpected discovery was made after 1998, which was awarded the Nobel Prize in Physics 2011. The Universe was found to expand with acceleration, and to describe it, either an analog of the Λ-term (a new form of matter dubbed dark energy) should be invoked, or GR should be generalized, for example, by introducing so-called $F(R)$ gravity, where the gravity is no longer identified with the curvature of spacetime but with a some function of this curvature. The question here arises: if such unexpected things occur when applying GR to the 'macroworld', are we guaranteed that new unexpected things will not emerge when making our efforts to penetrate into the 'microworld'? Therefore, we should indeed be cautious when reaching conclusions about the discovery of black holes. We should wait for the results of the RadioAstron mission, which offers the real possibility of conclusively proving the existence of black holes in nearby galactic nuclei.

The recent start-up of operations of large new 8–10-m optical telescopes has allowed the astronomers to study X-ray binary systems in other galaxies [27, 28], which can significantly increase the number of measured masses of neutron stars and black holes. This will improve the statistical significance of the observed difference in properties of these classes of relativistic objects.

Table 1. Parameters of X-ray binary systems with black holes *

System	Optical star spectrum	$P_{\rm orb}$, d	$f_{\rm v}(m)/M_\odot$	$v_{\rm rot}\sin i$, km s^{-1}	i, deg	$q = m_{\rm X}/m_{\rm v}$	$m_{\rm X}/M_\odot$	$m_{\rm v}/M_\odot$	a_*
Cyg X-1 (V1357Cyg) **	O9.7Iab	5.59983(2)	0.244±0.005	95±6	27.06±0.76	0.77±0.1	14.81±0.98	19.16±1.9	>0.95
LMCX-3 **	B3Ve	1.70479(4)	2.29±0.32	130±20	67±3	1.6±0.4	7.6±1.6	5±1	0.3±0.1
LMCX-1 **	O(7–9)III	3.90917(5)	0.14±0.05	129.9±2.22	37.0±1.87	0.34±0.07	10.3±1.3	30.6±3.2	$0.92^{+0.05}_{-0.07}$
RX J1826.2-1450 (LS5039) **	O6.5V((f))	3.90603(17) ($e = 0.35 \pm 0.04$)	0.0053±0.009	113±8	24.9±2.8	0.16±0.09	3.7±1.1	22.9±3.1	—
SS433 **	A7I	13.08211(10)	0.268±0.043	—	78.81±0.06	0.30±0.05	5±1 ****	15±3 ****	—
M33X-7 **	O(7–8)III	3.453014(20)	0.46±0.08	250±7	74.6±1.0	0.224	15.55±3.20	70.0±6.9	0.84±0.05
IC10X-1 **	WNE	1.4554	7.64±1.26	—	∼ 90	∼1.1	28±5 ****	26±9 ****	—
CygX-3 **	WN3-7	0.19968462(6)	0.027	—	> 60	—	∼ 10 ****	$\lesssim$70 ****	—
NGC300X-1 **	WN5	1.346(8)	2.6±0.3	—	68±7	∼0.87±0.2	17±6 ****	22±10	—
A0620-00 (V616Mon) ***	K5V	0.3230160(5)	2.72±0.06	83±5	51.0±0.9	16.5±3.0	6.60±0.25	0.40±0.045	0.12±0.19
GS2023 + 338 (V404Cyg) ***	K0IV	6.4714(1)	6.08±0.06	38.8±1.1	56±4	17.5±1.4	12±2	0.7±0.2	—
GRS1124-68 (GU Mus) ***	K(2–4)V	0.432606(3)	3.01±0.15	106±13	54±2	6.8±2	7.3±0.8	1.0±0.2	—
GS2000 + 25 (QZ Vul) ***	K5V	0.3440915(9)	5.01±0.12	86±8	64±1.3	24±5	7.5±0.3	0.3±0.1	—
GRO J1655-40 (XN Sco 1994) ***	F5IV	2.6219(2)	2.73±0.09	93±3	70.2±1.2	2.5±0.1	6.3±0.3	2.5±0.2	0.7±0.1
H1705-250 (V2107 Oph) ***	K5V	0.5222(44)	4.86±0.13	$\leqslant$ 79	> 60	>18.9	7.0±1.3	0.4±0.1	—
GRO J0422 + 32 (V518 Per) ***	M2V	0.2121600(2)	1.19±0.02	90±2.5	44±2	10±5	4.3±0.6	0.4±0.1	—
4U1543-47 (HL Lup) ***	A2V	1.116407(3)	0.25±0.01	46±2	20.7±1.5	3.6±0.4	9.4±1.0	2.6±0.3	0.8±0.1
GRS1009-45 (MM Vel) ***	(K6-M0)V	0.285206(2)	3.17±0.12	—	∼ 67 ****	7.2±0.9	4.2±0.6	0.6±0.1	—
SAXJ1819.3-2525 (V4641) Sgr ***	B9III	2.81730(1)	3.13±0.13	98.9±1.5	75±2	2.30±0.08	7.1±0.3	3.1±0.2	—
XTE J1118 + 480 ***	(K7-M0)V	0.169930(4)	6.1±0.3	114±4	81±2	26±3	6.8±0.4	0.3±0.02	—
GRS1915 + 105 ***	KIII	33.5	9.5±3.0	26±3	66±1	18±1.0	14±4	0.8±0.5	0.975±0.025
GX339-4 (V821Aql) ***	—	1.7557(4)	∼6.5	—	—	∼ 15	9±2	0.6±0.4	—
XTE J1550-564 ***	G8IV – K4III	1.5435(5)	6.86±0.71	90±10 ****	72±5	> 12	9.6±1.2	0.5±0.2	0.34±0.24
XTE J1859 + 226 ***	∼G5	0.382(3)	7.4±1.1	—	—	—	9.8±2.2	∼ 1	—
XTE J1650-500 ***	K4V ****	0.3205(7)	2.73±0.56	—	> 50	∼ 10 ****	$\leqslant$ 7.3 (4.0–7.3)	∼(0.4–0.7) ****	—
GS1354-64 *** (BWCir)	G(0–5)III	2.54451(8)	5.73±0.29	69±8	$\leqslant$ 79	8.3±3	$\geqslant$ 7.6	∼ 1 ****	—

* $P_{\rm orb}$ is the orbital period of the binary system, $f_{\rm v}(m)$ is the mass function, $v_{\rm rot}$ is the rotational velocity, i is the inclination angle of the binary orbital plane to the sky plane, $m_{\rm X}$ is the black hole mass, $m_{\rm v}$ is the mass of an optical companion, a_* is the dimensionless parameter of the black hole rotation, and $a_* = cJ/(GM^2)$.

** Stationary.

*** Transient.

**** Parameters to be confirmed in future studies. For references to original papers, see monograph [15].

New results have recently been obtained in studies of the rotation of stellar-mass black holes. As already noted in our review [4], the possibility of determining the angular momentum of a black hole stems from the fact that, if the black hole co-rotates with the accretion disk, the inner edge of the disk comes much closer to the black hole than in the case of a nonrotating black hole, since the radius of the event horizon of a rotating black hole is smaller than that of a nonrotating black hole. Therefore, the accretion-driven gravitational energy release, and hence the luminosity and temperature of a thermal X-ray emission from rotating black holes, should be larger than that from nonrotating black holes. This point was noted as early as the classical paper by I D Novikov and K S Thorne [11], who constructed the theory of disk accretion taking into account GR effects.

Several methods of determining the angular momentum of rotating black holes, including polarimetric X-ray observations of accreting black holes, are described in review [13]. If the mass of a black hole is known with a sufficient accuracy, the method based on the description of the X-ray spectrum of an accreting black hole utilizing the Novikov and Thorne model of a thin relativistic accretion disk [11] seems to be most accessible and quite reliable.

Thus far, angular momenta of nine stellar-mass black holes have been estimated (see Table 1). Of them, five black holes reside in low-mass transient X-ray binaries — X-ray novae (A0620-00, XTE J1550-564, GRO J1655-40, GRS 1915+105, 4U1543-47) [12], and four black holes are components of massive quasisteady X-ray binaries (LMCX-3 [29], M33 X-7 [30, 31], LMCX-1 [32], Cyg X-1 [33]). The measured values of the dimensionless angular momentum of these nine black holes lie within the range:

$$a_* = \frac{cJ}{GM^2} = 0.98 \text{ (system GRS1915+105)}$$
$$- 0.12 \text{ (system A0620-00)}.$$

Here, J is the black hole angular momentum, M is its mass, G is the Newtonian constant of gravitation, and c is the speed of light.

A remarkable result was recently obtained by R Narayan and J E McClintock [34]. They found a correlation between the observed radio fluxes from collimated jets from black holes, $P_{\rm jet}$, and the values of the dimensionless angular momentum a_* of the black holes (see Fig. 5):

$$P_{\rm jet} \sim a_*^2 .$$

This is the first observational evidence that the relativistic jets from accreting stellar-mass black holes can be generated from the conversion of the rotational energy of black holes into the kinetic energy of regular bulk motion of matter in collimated relativistic jets with outflow velocities close to the speed of light. Here, the well-known Blandford–Znajek mechanism seems to be operative [35].

Large values of the dimensionless parameter a_* for some black holes (for example, $a_* = 0.98$ for the $14M_\odot$ black hole in X-ray binary GRS 1915+105) suggest that these objects cannot be heavy neutron stars, since as the latter experience such a rapid axial rotation they would be disrupted by centrifugal forces. However, it should be borne in mind that values of a_* have been derived using GR formulas [11], so this conclusion is model-dependent. Relativistic collimated jets are observed in many X-ray binary systems (see, for example, review [4]). These X-ray binaries are called microquasars.

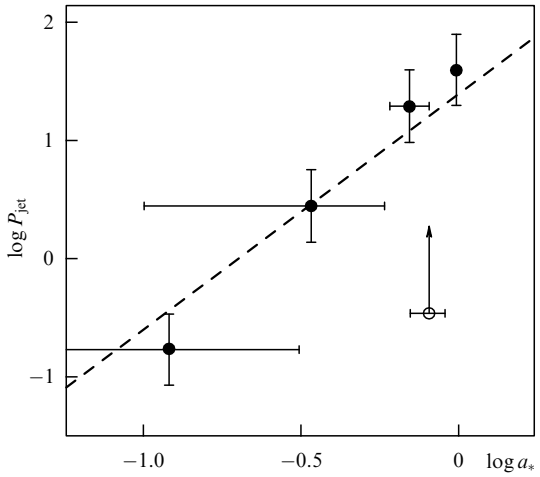

Figure 5. The power of relativistic jets $P_{\rm jet}$ from accreting black holes inferred from radio observations as a function of the dimensionless black-hole spin parameter a_* (taken from paper [34]). The dashed line corresponds to the theoretical dependence $P_{\rm jet} \sim a_*^2$ from paper [35].

Studies of microquasars are of special interest, since physical processes in microquasars are microscopic versions of processes occurring in quasars — very active galactic nuclei, as well as in the nuclei of other galaxies. Relativistic collimated jets are frequently observed from galactic nuclei. As the characteristic times of nonstationary processes in microquasars are comparatively short (from a few seconds to several months), these processes can easily be observed and studied. Then, the results of these studies can be employed to investigate quasars and nuclei of galaxies, where the characteristic nonstationarity times are much longer, so we observe these objects as if in a 'frozen' state.

4. Supermassive black holes in galactic nuclei

The first estimates of the masses of SMBHs in very active galaxy nuclei — quasars — were made as early as 1964 in the pioneering paper by Ya B Zeldovich and I D Novikov [36] under the reasonable assumption that the quasar luminosity is close to the critical Eddington luminosity.

Presently, the masses of SMBHs in galactic nuclei are estimated by assuming that the motion of 'test bodies' (gas disks, gas clouds, individual stars) near the black hole is governed by the gravitational field of the central black hole. Then, by equating the Newtonian gravity (attractive) force to the centripetal force, one can obtain the central SMBH mass:

$$M_{\rm BH} = \frac{\eta v^2 r}{G} , \qquad (2)$$

where v is the velocity of the test body, r is its distance from the central black hole, G is the Newtonian constant of gravitation, $\eta = 1-3$ is the factor that takes into account the character of the test body motion around the central black hole ($\eta = 1$ for circular motion). The test body mass is cancelled due to the equivalence principle — the equality between inertial and gravitating masses. Therefore, to find the black hole mass it is sufficient to know v and r.

The two most reliable methods of SMBH mass determination in galaxy centers are the resolved kinematics method and the reverberation method.

The method of resolved kinematics is based on direct observations of the motion of test bodies [37]. It can be applied to nearby galaxies, for which the telescope angular resolution allows 'watching' the test bodies residing in the galactic nucleus and direct measurement of their velocities and distances from the central black hole. As mentioned above, the resolved kinematics method enabled the mass of the central black hole in our Galaxy to be measured [3]. Using very long baseline radio interferometers, by the resolved kinematics method the mass of the SMBH in the center of NGC 4257 was reliably determined to be $M_{\rm BH} = 3.9 \times 10^7 M_\odot$ [38]. For more detailed results of SMBH mass estimations, see review [37] (see also Ref. [4]).

Unfortunately, the angular resolution of telescopes for the most of remote galaxies is insufficient to see individual test bodies; in these cases, one has to apply the reverberation method when estimating the mass of SMBHs. In this method, the velocities and distances of test bodies are determined indirectly. The velocity v is estimated from the Doppler width of emission lines formed in gas clouds rotating around the central black hole. The emission lines in the galactic nucleus spectrum are broadened due to the Doppler effect, so their half-widths characterize the mean velocity of motion of the emitting gas clouds. The characteristic distance r of the gas clouds from the central black hole is determined from the time delay of the emission lines' variability relative to that of the continuum spectrum which forms in the central parts of the galaxy nucleus. The time delay between the variability in emission lines relative to the continuum in active galactic nuclei was discovered in 1970–1972 [39]. It turned out that, although due to nonstationary processes in galactic nuclei both the lines and continuum change chaotically, a correlation is revealed between their changes: the line intensity variations repeat those of the continuum intensity with a time delay Δt, which in different galaxies varies from a week to several months (see Fig. 6). It was noted in paper [39] that a comparatively high gas density in the clouds implies a short gas thermal relaxation time, so the time delay Δt is basically the time of flight of hard emission photons, which are created near the central accreting source, to the gas clouds — test bodies emitting spectral lines. Then, the characteristic distance from the test bodies to the central SMBH can be estimate using formula $r \simeq c\Delta t$, where c is the speed of light. The black hole mass can ultimately be estimated from the known characteristic distance r and velocity v using formula (2). Starting from papers [40–42], the reverberation method for SMBH mass estimates has been widely applied to evaluate SMBH masses in active galactic nuclei [37].

There are also indirect, less reliable methods of SMBH mass estimates. These include, for instance, the use of widths and absolute intensities of emission lines in the active galactic nucleus spectra [43], the empirical relation between the black hole mass and velocity dispersion of stars in the galactic central regions, and the kink frequency in the power spectra of the X-ray irregular variability of galactic nuclei. Such methods enable a quick mass estimation of a large number of SMBHs, which is essential for statistical studies. As a rule, the results obtained with these indirect methods are calibrated by black hole masses which were reliably measured using resolved stellar kinematics and reverberation mapping. It should be specially emphasized that the first SMBH mass estimations in active galactic nuclei from spectroscopic data on emission line widths and absolute intensities were performed as early as 1982–1984 by E A Dibai [43]. The

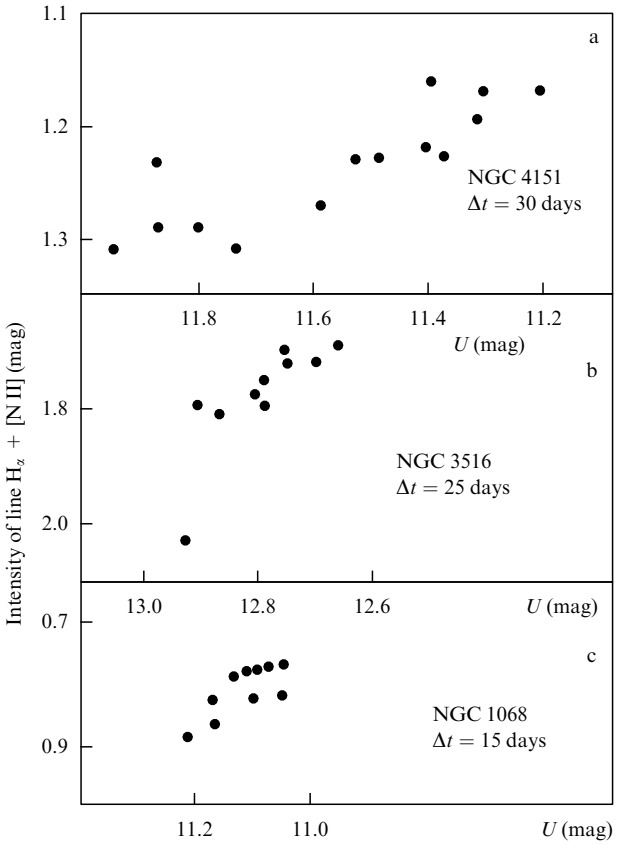

Figure 6. Correlation between the emission line H_α + [NII] and continuum spectrum intensities in nuclei of Seyfert galaxies NGC 4151 (a), NGC 3516 (b), and NGC 1068 (c) taking into account the time delay Δt of the emission line variability relative to the continuum; U (mag) is the stellar magnitude of the galactic nucleus in ultraviolet U filter. (Taken from paper [39]).

author of the latter study took advantage of the photoionization model of the active galactic nucleus in estimating the characteristic size of the emission line region. SMBH mass estimates given by Dibai are in reasonable agreement with modern results obtained from reverberation mapping.

To date, the masses of several hundred SMBHs have been measured applying resolved stellar kinematics and reverberation mapping techniques. They all lie within the range of $(10^6 - 10^{10})\, M_\odot$. The most reliable mass estimates of supermassive black holes in 44 ellipticals and 41 spirals (see the recent review by Kormendy and Ho [37]) span the interval from $(0.94 - 1.34) \times 10^6 M_\odot$ to $(0.49 - 3.66) \times 10^{10} M_\odot$. Here, the values in parentheses stand for the mass determination errors. Reliable values of masses of SMBHs and central star clusters were recently summarized by Zasov and Cherepashchuk [44] for 82 galaxies with known rotational velocities (i.e., with known total masses, including the dark matter halo mass).

Indirect mass evaluations were made for many thousand SMBHs in active galactic nuclei. For example, the targeted spectrophotometric Sloan digital sky survey (SDSS) allowed about 60 thousand SMBH masses in the centers of quasars (very active galactic nuclei) to be estimated by indirect methods, and the statistical dependence of SMBH masses on redshift to be constructed in the redshift range $z = 0.1 - 4.5$ [45] (see Fig. 7). It turned out that on average the SMBH mass increases with redshift (i.e., with a decrease in the proper age of a quasar). This effect, if free of a strong observational

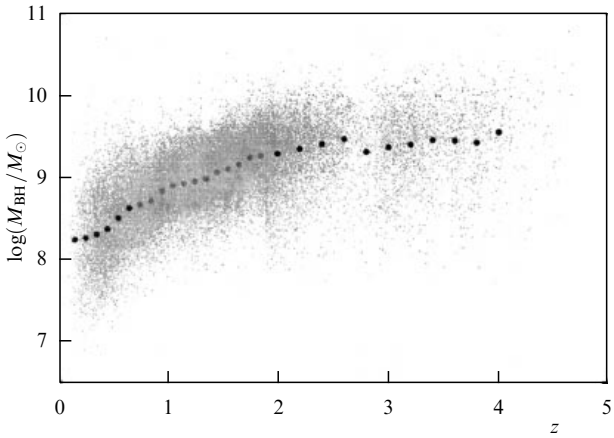

Figure 7. Masses of 60 thousand supermassive black holes in quasar nuclei as a function of redshift. (Taken from paper [45].)

selection, can hardly been explained in the framework of the model of an SMBH mass increase due to the accretion of circumnuclear matter in quasars. But the most difficult question to explain relates to the discovery of more than a dozen quasars with very high redshifts $z > 6$ and with the proper age of less than a billion years [46]. How could such massive ($M_{BH} = (10^8 - 10^9)\, M_\odot$) black holes be formed in a time of less than one billion years? This important observational fact poses a serious theoretical problem.

Recently, a careful account for observational selection effects was taken and a correction for data incompleteness was made by Kelly et al. [47] for 9886 quasars in the redshift range $1 < z < 4.5$. The authors of Ref. [47] stress that this correction is necessary, because the spectrophotometric SDSS survey for $z > 1$ is highly incomplete in the case of relatively low-mass black holes ($M_{BH} \leqslant 10^9 M_\odot$). Based on the corrected observational data for 9886 quasars, Kelly and his co-workers [47] constructed the mass distribution of SMBHs as a function of redshift z over the range $1 < z < 4.5$. The black hole mass function found in this way turned out to shift on average toward higher masses with increasing z.

A comparison of the observed black hole mass function derived in Ref. [47] with theoretical models of SMBH mass growth in galactic nuclei was drawn in Ref. [48]. The authors of the last paper tapped the model of SMBH mass growth based on the concept of hierarchical clustering, where the SMBH mass growth occurred through the coalescence of black holes with smaller masses and accretion of ambient gas at a fixed rate below the critical Eddington luminosity. Here, two types of SMBH seeds were employed: a low-mass seed (black hole with a mass of several hundred solar masses, formed from the core collapse of a population III first generation hydrogen–helium star), and a massive seed ($M = (10^5 - 10^6)\, M_\odot$) — a black hole resulting from the direct collapse of a pregalactic hydrogen–helium disk with low metal abundance. Models of such massive seeds are presented, for example, in paper [49]. The comparison of theory [48] with observations [47] led the authors of Ref. [48] to the conclusion that the low-mass seed model (population III stellar remnants) does not satisfactorily explain the observed black hole mass function for $M_{BH} > 10^9 M_\odot$ in the redshift range $1 < z < 4.5$. At the same time, the massive seed model permits us to adequately describe the observed black hole mass function for $M_{BH} > 10^9 M_\odot$ with the proviso that $z > 2$, and hence is favorable.

In recent years [50–55], the analysis of iron K_α line profiles in X-ray spectra of galactic nuclei has allowed the dimensionless angular momentum $a_* = cJ/(GM_{BH}^2)$ to be estimated for some black holes. These parameters were found to be less than the critical value of $a_* = 0.998$, in agreement with theoretical predictions [56]. The parameter a_* can be independently estimated from the kinetic energy flux in jets from SMBHs [57]. These estimates require the magnetic field value in the last stable orbit in the accretion disk [58] or on the SMBH event horizon [35] to be known. The group led by Yu N Gnedin [59–61] has derived a method for determining the magnetic field near SMBHs from spectropolarimetric observations of active galactic nuclei with account for the Faraday rotation of the plane of polarization along a mean free path of a photon scattered by plasma electrons in the accretion disk. Using spectropolarimetric observations of active galactic nuclei performed on the 6-m altazimuthal telescope BTA-6 of the Special Astrophysical Observatory (SAO) of the Russian Academy of Sciences (RAS) in B Zelenchuk (Caucasus) [62], estimates of the parameter a_* were obtained for more than a dozen SMBHs [63, 64]. The values found range from $a_* = 0.920 - 0.998$ to $a_* = 0.550 - 0.650$ (the dispersion characterizes the determination error) and does not exceed the theoretical upper limit, $a_* = 0.998$.

Limits on the radii of SMBHs are set by observations of fast variability of the optical, infrared, and X-ray emission from some galactic nuclei on time scales smaller than tens of minutes, which implies the upper bound $r < 20 r_g$ (see, for example, review [4]). Strong but model-dependent constraints on black hole radii can be obtained by analyzing the broadband X-ray profiles of the iron K_α emission line at 6.4 keV. The line width of this asymmetric component corresponds to velocities as high as $\sim 10^5$ km s^{-1}. The analysis of this component in the galaxy MCG 6-30-15 [65] implies that the inner edge of the accretion disk in this case is located at a distance smaller than $3r_g$ from the central SMBH, possibly due to its rapid rotation.

In the last few years, direct measurements of the radius of the black hole in the Milky Way center have been carried out using ground-based intercontinental radio interferometry at short wavelengths (≈ 1.3 mm) with an angular resolution of better than 10^{-4} arcseconds [66]. It is shown by direct observations of the galactic center [66] that the size of the emitting region around the SMBH with the mass of $4 \times 10^6 M_\odot$ is smaller than the size of its dark 'shadow'. Apparently, the innermost part of the rotating accretion disk moving toward the astronomer was observed [66], so that its brightness was enhanced due to relativistic effects. It cannot be ruled out, either, that the emission from the base of a relativistic jet forming near the black hole was recorded. In both cases, these observations [66] imply that the linear size of the SMBH in our Galaxy center is close to its gravitational radius. To find a conclusive validation of the assumption that the supermassive object in the center of the Galaxy is indeed a black hole, the authors of Ref. [66] plan to conduct radio observations with a very long base at shorter wavelengths ($\lambda < 1$ mm) and with a larger number of dishes. Should the challenging very long baseline interferometry of the galactic center at very short wavelengths be realized, it will increase the angular resolution and the 'signal-to-noise' ratio. The authors of Ref. [66] hope to obtain the image of the dark 'shadow' from the central SMBH and thus to conclusively prove its real black hole nature.

In this connection, the space radio interferometer RadioAstron, which possesses an angular resolution of better than 10^{-5} arcseconds at $\lambda = 1.3$ cm, has great potential.

Unfortunately, 10^{-5} cm is the shortest working wavelength of RadioAstron. To run through to the event horizon of the SMBH in our Galaxy center, observations at shorter wavelengths $\lambda < 1$ mm are required (at longer wavelengths, the radio wave scattering on plasma inhomogeneities in the galactic nucleus does not allow us to 'see' the close neighborhoods of the central SMBH [66]). However, in the case of the central black hole in the nucleus of M87 galaxy with mass $(3-6) \times 10^9 M_\odot$ [67, 68], the plasma density in the galactic nucleus must be significantly lower than in the nucleus of our Galaxy, and the galaxy itself is observed under a larger angle to the line of sight. Therefore, in this case one can hope to see the central SMBH shadow even at $\lambda = 1.3$ cm. The design of the Millimetron space radio interferometer mission, which is now under development by N S Kardashev's team, is the most suitable for such experiments. This interferometer will operate at very short radio wavelengths ($\lambda < 1$ mm) and is planned to have a huge angular resolution of down to 10^{-9} arcseconds, which is of fundamental importance for studies of SMBHs in the nuclei of many galaxies.

Thus, supermassive ($M_{\rm BH} = (10^6 - 10^{10})\, M_\odot$) and very compact objects with sizes not exceeding several gravitational radii) have been discovered to date in the nuclei of hundreds of galaxies. All their features most likely suggest that they comprise black holes.

5. Demography of stellar-mass and supermassive black holes

The large number of already discovered black hole candidates allows opening a new field of astrophysical research — black hole demography.

Black hole demography studies the formation and growth of black holes and their evolutionary connection to other astrophysical objects — stars, galaxies, etc.

In the last few years, a close similarity has been established between observational manifestations of black holes in X-ray binaries and in galactic nuclei [69]. In particular, the statistical dependence, called the fundamental plane, was discovered for supermassive and stellar-mass black holes [70]:

$$\lg L_{\rm R} = (0.60^{+0.11}_{-0.11})\, \lg L_{\rm X} + (0.78^{+0.11}_{-0.09})\, \lg M_{\rm BH} + 7.33^{+4.05}_{-4.07}\,, \tag{3}$$

where $L_{\rm R}$ is the observed radio luminosity (mainly due to relativistic jet radio emission), $L_{\rm X}$ is the X-ray luminosity (from the accretion disk and the jet base), and $M_{\rm BH}$ is the black hole mass (for both stellar-mass black holes and SMBHs).

The variability of active galactic nuclei containing accreting supermassive black holes was revealed to be similar to that of accreting stellar-mass black holes in X-ray binary systems if the variability time is normalized depending on the black hole mass [69]. It is well known that the X-ray variability of active galactic nuclei and black holes in binary systems can be described by the power spectral density $P(\nu)$ of variability, where ν is the frequency, and $1/\nu$ is the characteristic variability time. Over a large characteristic time, the function $P(\nu)$ can be described by a power law: $P(\nu) \sim \nu^{-\alpha}$, where $\alpha \approx 1$. Such a power law spectrum experiences a kink at shorter characteristic times, taking the form of $P(\nu) \sim \nu^{-\alpha}$, with $\alpha \geqslant 2$. The corresponding kink frequency in the spectrum is denoted as $\nu_{\rm B}$, and the characteristic time of the spectral kink is $T_{\rm B} = 1/\nu_{\rm B}$. Then, if $T_{\rm B}$ and $L_{\rm bol}$ (luminosity characterizing the accretion rate) are known from observations, the black hole mass $M_{\rm BH}$ can be estimated from the relationship

$$\lg T_{\rm B} = 2.1 \lg M_{\rm BH} - 0.981 \lg L_{\rm bol} - 2.32\,. \tag{4}$$

We stress that this statistical dependence is valid for both stellar-mass black holes and SMBHs. Accreting black holes in binary systems demonstrate aperiodic X-ray variability on time-scales from several days to $10^{-2} - 10^{-3}$ s. Such variability is also observed in the emission from accreting SMBHs but on much longer time-scales — from several years to several months or weeks.

In X-ray binaries with black holes, in addition to irregular variability, there are two types of quasiperiodic (i.e., not strictly periodic) oscillations (QPOs) of an X-ray flux: low-frequency QPOs (LFQPOs) with the characteristic frequencies of 0.1–30 Hz, and high-frequency QPOs (HFQPOs) with frequencies falling in the range of 40–450 Hz (see, for example, Refs [12, 13]). Low-frequency QPOs can be observed for several days or even months. For example, LFQPOs with frequencies of 2.0–4.5 Hz were observed over six months in the black-hole binary GRS 1915 + 105 in 1996–1997. In addition, this system experienced HFQPOs with frequencies of 41 and 67 Hz, as well as with 113 and 168 Hz. Attempts to connect low-frequency QPOs with the geometrical and physical characteristics of accreting plasma meet with difficulties, since an LFQPO corresponds to frequencies which are much lower than those corresponding to inner orbits in the accretion disk (where most of the X-ray emission is generated). For example, the orbital frequency of 3 Hz corresponds to the accretion disk orbit radius for a $10 M_\odot$ black hole at about $100 r_{\rm g}$, while the assumed size of the disk region with maximum X-ray energy release falls in the interval $(1-10)\, r_{\rm g}$, depending on the black hole spin. Numerous models of LFQPOs suggest different mechanisms of accretion disk oscillations (see, for example, Ref. [71]).

High-frequency QPOs are directly related to processes proceeding near the last marginally stable orbit around the black hole, since the orbital frequency in the last marginally stable orbit, according to Ref. [13], equals 200 $(M/(10 M_\odot))^{-1}$ Hz for a Schwarzschild black hole, and 1615 $(M/(10 M_\odot))^{-1}$ Hz for a rapidly rotating Kerr black hole. Remarkably, HFQPOs emerge in pairs in some cases with the frequency ratio 3:2. Examples of such black-hole X-ray binaries include GRO J1655-40 (300, 450 Hz), XTE J1550-564 (184, 276 Hz), GRS 1915 + 105 (113, 168 Hz), and H1743-322 (165, 241 Hz). In GRS 1915 + 105 binary system, the second pair of HFQPO (41, 67 Hz) is observed with frequencies which are not in the 3:2 ratio.

The 3:2 ratio for HFQPOs can evidence that these QPOs are due to some resonance phenomena in oscillations involving the innermost parts of accretion disks around black holes, which are described by GR (see, for example, Refs [72–74]). As noted in paper [12], the empirical relation between the HFQPO frequency and black hole mass in X-ray binaries arises:

$$f_0 \approx 931 \left(\frac{M_{\rm BH}}{M_\odot} \right)^{-1} \text{Hz}\,,$$

where f_0 is the fundamental frequency of the frequency pair, so that the observed frequencies are $2f_0$ and $3f_0$.

Quasiperiodic X-ray oscillations were recently discovered from accreting SMBHs in the nuclei of some galaxies. For example, QPOs with the characteristic period of about one hour were observed in the active nucleus of galaxy RE J1034+396 [75]. With a central black hole mass of about $10^7 M_\odot$, this quasiperiod corresponds to an orbit radius of about $3r_g$, which yields an upper limit on the size of this very massive and compact object, giving support to its black hole nature.

Interesting results were obtained in studies of the mass distribution of stellar-mass black holes.

It turned out that in binary systems there is no dependence of masses of relativistic compact objects on their companion masses [4]. Both neutron stars and black holes are found in binaries with both high-mass and low-mass companions. The black-hole mass in a binary system is also found to be independent of the mass of its binary companion. In this respect, close binaries with neutron stars and black holes are similar to classical close binaries in which, as was many times stressed by D Ya Martynov [76], any combinations of component masses occur.

The neutron star and black-hole mass distributions turned out to be unusual as well [77, 78] (see Fig. 8). The number of studied stellar-mass black holes does not increase with decreasing their mass. This looks strange, since the stellar mass distribution in the Galaxy (the most massive stellar objects are progenitors of the relativistic compact stars) is such that the number of stars very strongly (as M^{-5}) increases with decreasing stellar mass. As stellar-mass black holes originate from collapses of iron cores of massive ($M > 30M_\odot$) stars, the number of lower mass black holes should apparently strongly increase, but this is not observed (see Fig. 8). It can be shown [4, 79] that this unusual fact is not due to observational selection effects (for example, the disruption of a stellar binary during a supernova explosion or the mass loss via stellar wind from the massive star — the progenitor of a relativistic object, etc.). In addition, a mass distribution dip between $2M_\odot$ and $4M_\odot$ seems to exist for neutron star and black hole masses. In this mass range, no neutron stars or black holes have been observed. The mass dip within the range of $(2-4)\,M_\odot$ for neutron star and black hole mass distributions, if confirmed in further observations, will require a serious theoretical elucidation.

In this connection, it is worth mentioning one interesting possibility of explaining the unusual black-hole mass distribution. In paper [80], the hypothesis was put forth that the observed flat black-hole mass distribution and the $(2-4)\,M_\odot$ mass dip may be due to enhanced quantum evaporation of black holes, as suggested by some multidimensional models of gravitation (see, for example, Ref. [81]). In these models, the quantum evaporation time of a black hole can be much shorter than the Hawking time [82] and the former may be evaluated according to the formula

$$\tau \sim 1.2 \times 10^2 \left(\frac{M_{\rm BH}}{M_\odot}\right)^3 \left(\frac{1\ \text{mm}}{L}\right)^3 \text{years}\,,$$

where L is the characteristic scale of the additional (fourth) space dimension. With the mean black-hole mass of $\sim 9M_\odot$ and the expected upper limit of the scale L reaching a few hundredths of a mm, the quantum evaporation time prevails at a range of $10^8 - 10^9$ years, which is less than the age of the Universe and is comparable to the nuclear timescale of stellar evolution. As the quantum evaporation rate strongly (as M^{-3}) increases with decreasing black-hole mass, it may be inferred that the observed deficit of low-mass black holes and the $(2-4)\,M_\odot$ mass dip in the mass distribution of relativistic objects are concerned with the fact that many black holes with a relatively small masses has had time to evaporate in a Hubble time.

It is notable that the mean observed mass of $9M_\odot$ of a stellar-mass black hole allows us to impose the restriction in this model on the size of the space extra dimension L, which is in agreement with laboratory constraints [83]. On the other hand, if the quantum evaporation time of a stellar-mass black hole is smaller than the age of the Universe (1.4×10^{10} years), the decrease in the mass of a black hole in an X-ray binary system should lead to the observed variation of its orbital period. Searches for such orbital period changes in X-ray

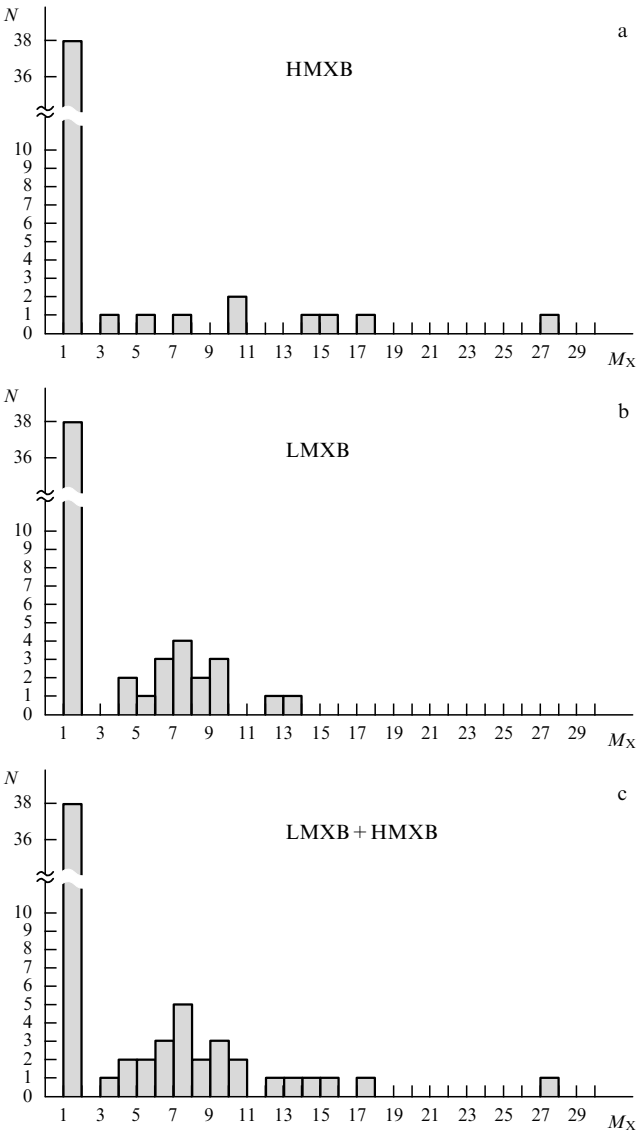

Figure 8. Neutron star and black-hole mass distributions in binary systems: (a) black-hole masses in high-mass X-ray binaries (HMXB) with optical O–B and WR companions; (b) black-hole masses in low-mass X-ray binaries (LMXB), and (c) the total black-hole and neutron star mass distributions (in low-mass and high-mass X-ray binaries). The high peaks in the left parts of panels (a)–(c) correspond to neutron star masses.

binaries with black holes are under way. The results of these studies allowed imposing the upper bound on the characteristic size of space extra-dimension (fourth) scale: $L < 0.1$ mm [84]. As the precision of measurements of orbital periods of binary systems increases with the number of orbital cycles, further accumulation of observational data on the orbital periods in X-ray binaries can significantly improve this estimate.

There are other, less exotic explanations of the anomalous black hole mass distribution in binary systems, which are related, for example, to the mass loss via stellar winds from massive stars [77], as well as to peculiarities of the late stages of massive star evolution [85–87]. The authors of these studies conclude that the mass of a black hole resulting from massive star core collapse is determined not only by the stellar core mass, but other characteristics as well, such as the rotation of the core, its magnetic field, and different instabilities that can be developing during the core collapse, and so forth.

Recently, the idea has arisen that collapses of carbon–oxygen cores of fast axially rotating Wolf–Rayet stars, leading to the formation of extremely fast rotating (Kerr) black holes in different galaxies, may be responsible for triggering the famous and yet enigmatic cosmic gamma-ray bursts in which a huge energy, comparable to a sizable fraction of the solar mass annihilation energy, is released in a few seconds. As noted in paper [88], the orbital motion of a nearby companion in a very close binary system can tidally sustain the fast axial rotation of the star, in spite of a significant loss of angular momentum associated with the outer shell ejection during a supernova explosion. The rapid axial rotation of the collapsing stellar core leads to the formation of a rapidly rotating (Kerr) black hole with collimated relativistic jets. These jets penetrate the stellar envelop and carry out gamma-ray emission from the central parts. Therefore, it is possible that by observing so-called long gamma-ray bursts we directly 'see' the process of formation of very rapidly rotating stellar-mass black holes in very close binary systems.

Let us briefly discuss the problem of SMBH demography. A lengthy discussion of this problem, based on statistical studies of 85 galaxies with the most reliably measured masses of central supermassive black holes (applying the resolved kinematics method), can be found in the recent review by Kormendy and Ho [37]. As noted in Section 4, the formation time of SMBHs in galactic nuclei is relatively short, namely less than one billion years. This conclusion is supported by the discovery of a dozen quasars with very high redshifts $z > 6$. Recently, a very massive black hole with a mass of $4 \times 10^{10} M_\odot$ was suspected to reside in the center of the galaxy (the proper age of this galaxy is about one billion years) with redshift $z \simeq 3.4$ [89].

Such a rapid formation of very massive black holes is difficult to explain in the models assuming their mass growth due to gas accretion onto a low-mass seed black hole that has been formed via the core collapse of a massive ($M = (100-1000)\, M_\odot$) population III star, even if the mass accretion rate is as high as the Eddington luminosity (see Section 4). Because the black hole mass of forty billion solar masses corresponds to almost half the baryonic mass of our Galaxy, some researchers are seriously discussing the question of what comes first — the galaxy formation at the early evolutionary stage of the Universe with the subsequent formation of an SMBH in its center, or the formation of the primary supermassive black hole that accretes baryonic matter from which galactic stars later form.

In our review [4], the main statistical relationships between the mass of the central SMBH and the host galaxy parameters were described. To date, most of these correlations have been confirmed, improved, and substantiated using rich observational data. In particular, SMBHs were found to correlate in a different way to distinct galactic components (bulges, pseudobulges, and disks) [37]. Starting from 2006, using the 6-m telescope of SAO RAS, our group at Sternberg Astronomical Institute (Moscow) has been carrying out observations of rotational velocities and velocity dispersions of stars and gas in galaxies with well-measured masses of central supermassive black holes [90, 91]. These observations allow us to study the relationship between the central SMBH mass and the kinematic characteristics of the galaxies and their structures. It is important that the galactic rotation enable the total mass of the galaxy, including baryonic and dark matter (the last mass can be ten times as heavy as the baryonic mass), to be estimated. The almost linear dependence revealed in Ref. [92] between the SMBH mass in the galactic nucleus and that of the galactic bulge (spherical crowding of old low-mass stars with high velocity dispersion close to the nucleus) was confirmed [91, 93].

A new intriguing fact has also emerged: the ratio of the central SMBH mass to the galactic bulge mass tends to increase with redshift, i.e., with a decrease in the proper galaxy age [94].

Recently, in addition to SMBHs, the important role of massive stellar clusters located in galaxy centers has been revealed [91, 95, 96]. Although observational selection effects can be important here, it is becoming evident that SMBHs exist in galaxies with massive spheroidal stellar components (for example, in massive elliptical galaxies or early type spirals with massive bulges, $M_{\rm sph} \gtrsim 10^{10} M_\odot$). Apparently, SMBHs tend to avoid most of the galaxies without a massive stellar spheroid component (see, for example, Refs [97, 98]). In galaxies with intermediate-mass spheroidal stellar components ($10^8 M_\odot \lesssim M_{\rm sph} \lesssim 10^{10} M_\odot$), both SMBHs and massive stellar clusters of comparable mass can be found (see, for example, Refs [99, 100]). An important correlation is also revealed between SMBH masses, the masses of central star clusters, and the parameters of spheroidal galactic components:

$$M \sim \sigma^\beta ,$$

where M is the mass of the SMBH or a stellar cluster, and σ is the star velocity dispersion in the spheroidal component. The index of a power is $\beta = 4-5$ for SMBHs (see, for example, Ref. [101]), and β falls within the range from 1.57 ± 0.24 [101] to 2.73 ± 0.29 [97] for massive central star clusters. Although the dispersion of the exponent β for central star clusters is large ($\beta = 1.57-2.73$), the dependence of mass on the velocity dispersion σ for central star clusters may be considered as weaker and better corresponding to the virial theorem ($\beta = 2$) compared to SMBHs. This allows us to assume that the formation and evolution of central SMBHs and massive star clusters in galactic nuclei are related to different mechanisms.

Of special interest is the possible association of central SMBHs and massive star clusters with dark matter in galaxies. Our observations of the galactic rotation in galaxies with known heavy central black-hole masses are aimed at solving this problem [90, 91, 44]. As shown in studies performed by A V Gurevich's group [102], the gravitational instability in proto-galaxy dark matter clumps form sharp and deep minima of gravitational potential (cusps), into

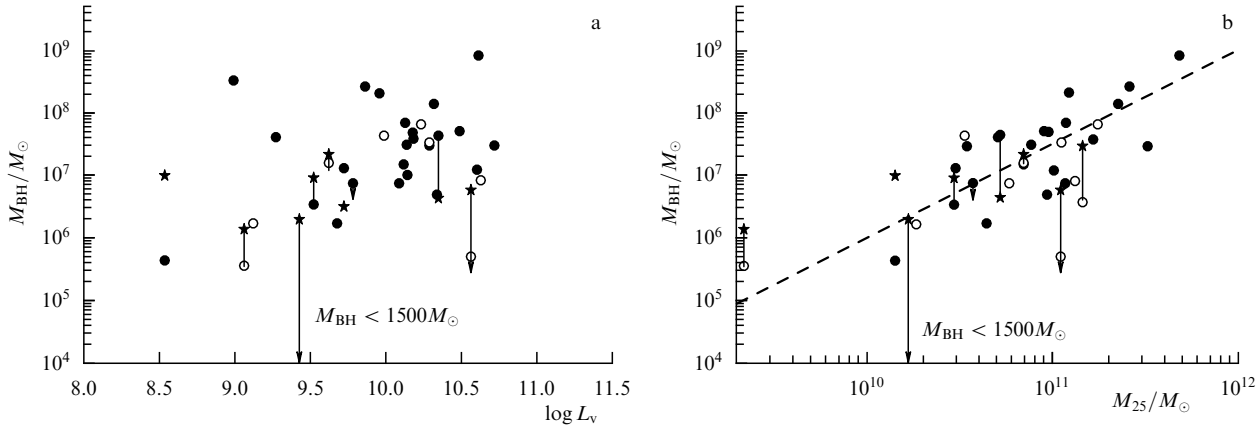

Figure 9. SMBH mass as a function of: (a) total optical luminosity L_v of the host galaxy characterizing the baryonic mass, and (b) the indicative mass of the galaxy $M_{25} = V_{far}^2 R_{25}/G$, which includes both baryonic and dark-matter masses. The filled 'star' symbols correspond to central stellar clusters. Linear segments join circles (black holes) and stars (clusters) in one galaxy. Arrows show the upper mass limits. (Taken from paper [91].)

which baryonic matter 'falls' to produce a stellar population of the forming galaxy.

This process can also stimulate the formation of an SMBH in the galaxy nucleus. Therefore, the association of the central SMBH mass with the mass of the galactic halo dominated by dark matter is rather expectable. Indeed, due to coalescence of galaxies at early stages of their formation, as well as star formation in galactic centers, this association can be rather indirect. Nevertheless, the search for a correlation between the central SMBH mass and the dark matter-dominated galactic halo mass is a very important observational task. The relation between the SMBH mass and the virial mass of the galaxy (as inferred from its rotation) is predicted in some numerical cosmological simulations [102–105].

The first indications of such a correlation were found by Baes et al. [106], where the following approximate dependence was developed:

$$M_{BH} \sim M_{halo}^{1.27}\,.$$

In paper [106], the SMBH masses and the galaxy maximum rotational velocities were indirectly estimated in most cases by utilizing data on the star velocity dispersion in the galaxies. That is why, the surprisingly strong correlation between M_{BH} and M_{halo} found in Ref. [106] may be due to correlated methods of determining SMBH mass M_{BH} and the galaxy maximum rotational velocity V_{far}. In our paper [107], the $M_{BH}(M_{halo})$ correlation was examined for the first time by invoking reliable direct SMBH mass measurements (made by the resolved kinematics and reverberation methods) and directly observed Galaxy rotational velocities V_{far}. In this case, both M_{BH} and M_{halo} are determined completely independently. The $M_{BH}(V_{far})$ and $M_{BH}(M_{halo})$ correlations turned out to be much less strong in this approach than those found earlier [106]. Thus, the association between the SMBH mass and galactic halo mass appears to be highly indirect. In addition, it was found [107] that the central SMBH mass at one and the same galaxy maximum rotational velocity, was higher in galaxies with heavier (baryon-dominated) bulge masses, suggesting a two-parametric relationship:

$$M_{BH} \sim M_{BH}(M_{halo}, M_{bulge})\,.$$

Correlations obtained in our paper [91] are presented in Fig. 9. They demonstrate the important role of dark matter in the central SMBH formation in the galactic nucleus. This figure depicts two dependences: $M_{BH}(L_v)$ and $M_{BH}(M_{25})$, where L_v is the total optical luminosity of the galaxy, which is a single-valued function of the total baryonic mass of the galaxy, and M_{25} is the so-called indicative mass of the galaxy: $M_{25} = (V_{far}^2 R_{25})/G$, where V_{far} is the observed maximum rotational velocity of the galaxy (which tends to a plateau at large distances from the nucleus), and R_{25} is the radius of the galactic region limited by the surface brightness isophot reaching the 25th stellar magnitude per square arcsecond, which determines the boundary of the visible part of the galaxy. Apparently, there is virtually no correlation between the SMBH mass and the total baryonic mass of the whole galaxy. At the same time, if we consider the indicative galactic mass M_{25} for the same galaxies as comprising both baryonic and a substantial fraction of dark matter, a good $M_{BH}(M_{25})$ correlation is revealed. This result immediately indicates that the influence of dark matter on the central SMBH formation, although indirect, remains quite significant. This conclusion can be interesting for theoretical studies of SMBH formation in galactic nuclei (see, for example, Ref. [102]).

A good correlation was also found in paper [91] between the central SMBH mass and galactic rotational velocity at the distance $R = 1$ kpc from the galaxy center, which characterizes the dynamically and/or chemically isolated core region in disk galaxies (see Fig. 10). Since the mean density in the inner galactic region within the radius R is proportional to the square of the rotational angular velocity at this distance, the presence of correlation in Fig. 10 suggests an association between the central SMBH mass and the mean density of matter in the galaxy interior. In paper [91], based on the idea suggested by Baes et al. [108] and on the model posed by Xu et al. [109] about the monolithic collapse of matter during formation of the inner parts of galaxies, the hypothesis was put forward that it is the monolithic collapse of pseudoisothermal gas in the region with the characteristic radius $R \simeq 1$ kpc that is responsible for the rapid formation of both the central SMBH and the 'classical' bulge at the early stage of the galaxy formation. The formation of SMBHs and central massive star clusters seems to occur on different time scales, and the masses of nuclear star clusters (if they could be

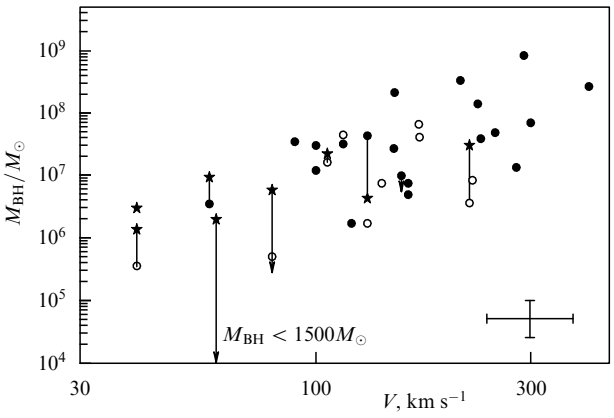

Figure 10. Correlation between the SMBH mass M_{BH} and the galaxy rotational velocity $V(R)$ at a distance of $R = 1$ kpc from the galactic center. Notations are the same as in Fig. 9. Characteristic errors are shown in the bottom right corner. (Taken from paper [91]).

formed near the SMBH) apparently continue to increase after cessation of the SMBH growth.

The linkage of central SMBHs and stellar clusters with the kinematics and color of host galaxies was studied in more detail [44]. In particular, it was revealed that the mass of the central star cluster, M_{nc}, stronger than the SMBH mass M_{BH} correlates with the kinematic parameters and mass of the galactic disk, as well as with the total mass of the galaxy. Lenticular galaxies have, on average, higher masses M_{BH} than galaxies of other types, all other conditions being equal. A tighter association of the mass M_{nc} with the dark galactic halos allows us to assume that the potential well produced by the central dark matter density peak (cusp), which can be smoothed out by active star formation, will determine the growth rate of the central star cluster in the young galaxy. The conclusion that SO-Sb galaxies with a weak star formation (which have a 'red' color) excel in more massive central black holes agrees well with the scenario in which the separation of galaxies into two sequences ('blue' and 'red') is due to a significant loss of gas by the galaxy at the stage of high activity of its nucleus (supercritical accretion of gas onto the central SMBHs) if the massive central black hole with mass $M_{BH} > (10^6 - 10^7)\, M_\odot$ is present. The corresponding gas sweeping from the galaxy caused by its nucleus activity should not lead to the disruption of the central star cluster.

6. High angular resolution experiments

Direct imaging of a black hole could be the most compelling evidence of its reality. Clearly, it is impossible to observe an isolated classical black hole because it does not emit radiation. In real astrophysical conditions, however, both stellar-mass black holes and SMBHs are surrounded by accreting disks, in which energy is released due to matter accretion. As noted in Section 4, the black hole should be observed as a dark spot (shadow) against the bright background of inner parts of the geometrically thin accretion disk, since any signal, including electromagnetic radiation, cannot escape from the black hole to the space infinity. Due to gravitational lensing effects, the typical size of the shadow is 2.6 times as large as the double gravitational radius of the black hole [110, 111]. Moreover, photons from the accretion disk near the event horizon not only change the trajectory, but can also be captured by the black hole gravitational field to revolve many times around it [112, 113]. This is one of the reasons for the increase in the visible size of a black hole shadow.

The diameter and shape of the BH shadow can be calculated in GR using the ray tracing method along geodesic lines in the black hole spacetime (see, for example, Refs [114, 115]). According to Takahashi and Watarai [115], applying the low-efficiency radiative model ADAF (Advection Dominated Accretion Flow), in which advection onto the black hole dominates, permits calculating the emission at wavelengths $\lambda \leqslant 1$ mm from the black hole in our Galaxy center (the radio source SgrA*), which is dominated by synchrotron radiation of thermal electrons in a magnetic field. The light rays from the inner parts of the low-efficiently radiating accretion disk are strongly bent in the black hole gravitational field, absorbed and scattered in the surrounding plasma. These absorption and scattering in the interstellar medium additionally increase the effective size of the black hole visual image, which varies proportionally to λ^2. Therefore, as noted above, the true black hole shadow in the center of our Galaxy should be observed at short wavelengths with $\lambda < 1$ mm [66]. The brightness of rapidly rotating inner parts of the accretion disk is distributed asymmetric due to relativistic aberration effects (including the Doppler effect and possibly reference frame dragging in the rotational black hole spacetime). The shape of the shadow also becomes asymmetric due to relativistic frame dragging [112, 114]. In addition, the image of the base of the relativistic jet formed in the inner parts of the accretion disk can be projected onto the black hole shadow [116].

Dexter et al. [116] reported calculation of the structure of the nearest neighborhood of the supermassive black hole in the center of the M87 galaxy with a collimated relativistic jet. According to recent measurements [68], the SMBH mass in M87 is equal to $6.4 \times 10^9 M_\odot$, which is two times as high as the previous estimate obtained in the pioneering paper by Ford et al. [67]. This mass value is ~ 1600 times as high as the black hole mass in the center of our Galaxy. Therefore, the Schwarzschild angular radius of the central black hole in M87 galaxy at a distance of 16 Mpc is about 4/5 of that of the black hole in the center of our Galaxy (see Table 2). This makes the M87 galaxy very suitable for direct measurements of the black hole radius (more precisely, of its shadow) by methods of space and even ground-based intercontinental radio interferometry at short wavelengths ($\lambda \lesssim 1$ mm).

The authors of paper [116] emphasize that the dark shadow from this SMBH, providing direct evidence for the existence of the event horizon, can be literally 'seen' in the nearest future using short-wavelength very long baseline interferometry (VLBI), for example, involving radio telescopes in the Hawaii islands and in the vicinity of Mexico City. The authors of Ref. [116] calculated the visible structure of the vicinity of the SMBH in the M87 center for two models: with radiation dominated by the accretion disk, and with radiation dominated by a jet. An important conclusion of paper [116] resides in that radiation emission from the counterjet can dominate in the emission around the black hole shadow in M87 due to its low spin axis inclination to the line of sight (25°), while the radiation from the forward jet can be strongly weakened due to gravitational capture of photons by the black hole (see Fig. 11).

Table 2 lists the masses of some stellar-mass and supermassive black holes, their distances, and the corresponding

Table 2. Masses of black holes, their distances, and diameters of shadows for different black hole masses.

Object	Mass/$M_\odot$	Distance, kpc	Schwarzschild radius			Shadow diameter, μarcseconds
			(cm)	(A.U.)	(μarcseconds)	
Stellar-mass black hole	10^1	1	2.95×10^6	1.97×10^{-7}	0.0002	0.001
SgrA*	4.1×10^6	8	1.09×10^{12}	7.28×10^{-2}	9.10	45.48
M31	3.5×10^7	800	1.03×10^{13}	6.88×10^{-1}	0.86	4,30
NGC 4258	3.9×10^7	7200	1.15×10^{13}	7.76×10^{-1}	0.11	0.53
M87	6.4×10^9	16,100	1.89×10^{15}	1.26×10^2	7.82	39.08

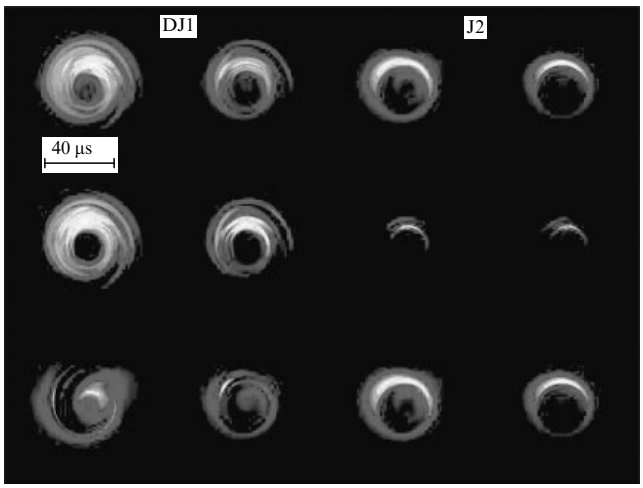

Figure 11. Model images of the vicinity of the central SMBH in M87 galaxy from paper [116]. The black hole shadow is seen against the background of emission of the accretion disk and jets. Two models are used in calculations: with accretion disk-dominated radiation (two left columns), and with jet-dominated radiation (two right columns). In each pair of columns, the left and right columns correspond to observations at $\lambda = 1.3$ mm and $\lambda = 0.87$ mm, respectively. In the disk-dominated model (two left columns), the disk radiation and weak forward jet emission are seen, while the emission from the counterjet is absorbed by the accretion disk. In the jet-dominated model (two right columns), the emission from the counterjet enhanced by light-ray bending in the strong gravitational field of the black hole dominates, while the emission from the forward jet is strongly weakened by acting the strong gravitational field of the black hole. The upper row corresponds to the disk + jet structure, the middle row to the disk, and the bottom row to the jet.

linear and angular sizes of their shadows. It is seen that the expected angular size of the shadow from a galactic stellar-mass black hole is very small ($\sim 10^{-9}$ arcseconds), which is marginally detectable even by the unique planned space radio interferometer Millimetron. However, the angular shadow sizes from the central SMBH in the Milky Way nucleus and in the nuclei of some nearest galaxies are quite large: $\sim 5\times10^{-5}-5\times10^{-7}$ arcseconds, which is reachable by the space interferometer RadioAstron and planned Millimetron space mission. For example, the angular size of the shadow from the Milky Way central SMBH ($M\simeq4\times10^6 M_\odot$) is $\sim 5 \times 10^{-5}$ arcseconds, and for the SMBH with mass $6 \times 10^9 M_\odot$ in M87 it is $\sim 4 \times 10^{-5}$ arcseconds. As noted in Section 4, there is hope to reach the 10^{-5}arcsecond angular resolution even by applying the standard VLBI radio interferometry at short wavelengths ($\lambda < 1$ mm) [66].

The diameter and shape of the BH shadow depend on the black hole mass and angular momentum [115]. If the mass of an SMBH is known from independent measurements (for example, it was derived from the motion of nearby stars) and its angular momentum was also estimated independently (for example, from the iron line profile in the X-ray spectrum), then a comparison of the model size and shape of the calculated shadow with observed values can be used to get the conclusive quantitative proof of the presence of a black hole in the galaxy center.

High angular resolution spectroscopy also enables the accretion disk brightness distribution in the nearest vicinity of a black hole to be investigated and, moreover, different nonstationary processes in the accretion disk interior and at the base of the relativistic jet to be studied. According to Ref. [117], the advection-dominated regime ADAF in the accretion flow of matter is subject to thermal instability. If the ADAF regime occurs in the inner regions of the accretion disk, plasma density clumps and hot spots can appear near the black hole horizon, causing short-term variability of emission on timescales of the order of several dozen minutes (for an SMBH). For example, the short-term variability of infrared and X-ray emissions is actually observed from SgrA* in our galactic center [118]. Presumably, the motion of bright spots in the parts of the accretion disk nearest to the event horizon can impose additional constraints on the spacetime metric near the black hole.

Figure 12 displays the image of the BH shadow and nearest neighborhood of the accretion disk theoretically calculated for the SgrA* source in the galactic center [119]. In this case, the black hole shadow is seen against the bright accretion disk background. The possible contribution from the relativistic jet is neglected. The black hole mass in the Milky Way center is of order $4 \times 10^6 M_\odot$ (see Section 1). The figure shows the black hole shadow and complicated brightness distribution around it: the left part of the accretion disk, in which matter moves with a near-luminous velocity, approaches the observer, is brighter due to relativistic aberration, and has a higher brightness temperature than the right part, which recedes the observer. The glowing 'halo' around the shadow is observed even when the line of sight lies close to the accretion disk plane. This is due to light rays bending in the strong black hole gravitational field, which enables even the rear side of the disk from behind the shadow to be seen. In addition, photons emitted by the rear part of the accretion disk are bent in the black hole gravitational field so strong that they move near the shadow along closed trajectories.

The assumed structure of nearby regions around the SMBH with mass $6 \times 10^9 M_\odot$ in the center of the M87 galaxy [116] is depicted in Fig. 11. Recently, the results of observations of the central parts of M87, obtained by intercontinental radio interferometry at the short wavelength of 1.3 mm with an angular resolution of about 10^{-5} arcsecond, were reported

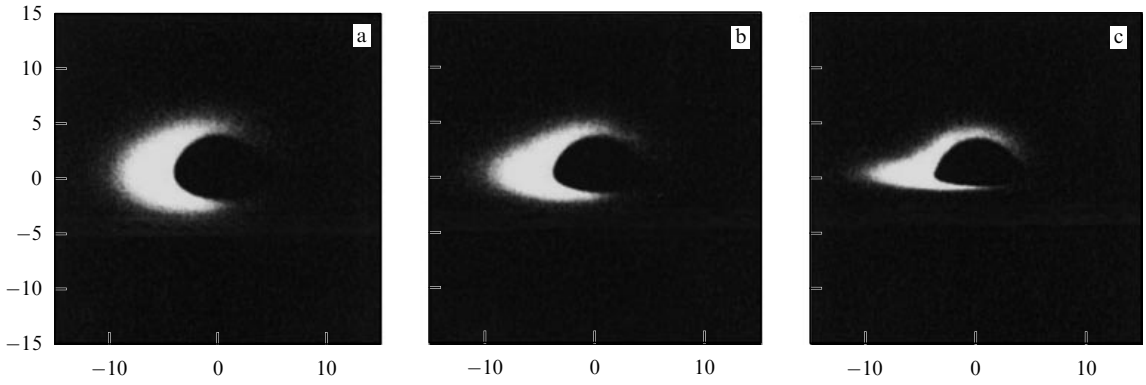

Figure 12. Image of the galactic center which the observer 'would see' using an interferometer with an angular resolution of $\sim 10^{-6}$ arcseconds at short radio waves for the disk inclination angle to the sky plane $i = 60°$ (a), 70° (b), and 80° (c). The x-axis and y-axis show the declination and right ascension in fractions of the Schwarzschild radius of the black hole. The inner bright parts of the accretion disk and the supermassive black hole shadow are seen. (Taken from paper [119].)

[120]. The measured diameter of the luminous region around the SMBH is about 5.5 ± 0.4 Schwarzschild radii. The authors invoked two models for estimating the angular size of the luminous region around the black hole: the radial Gaussian brightness distribution, and Gaussian brightness distribution in the outer parts with a strongly decreased intensity in the center (which models the presence of the central black hole shadow). It turned out that both models provided a good fit to radio interferometric observations. It is important that the model with the black hole shadow not be rejected by observations. Further data accumulation in this program (which the authors call the Event Horizon Telescope) will allow us to conclusively establish the nature of the supermassive compact object in the center of the M87 galaxy.

Tidal disruption of stars passing near an SMBH, predicted by M J Rees [121], can also lead to the formation of bright variable structures near the event horizon. As shown in papers [122, 123], when a star passes in the immediate vicinity of a not very massive black hole ($M_{\rm BH} < 10^8 M_\odot$), the following sequence of events occurs: the tidal deformation of the star; its disruption by black hole tidal forces, the fall of matter onto the black hole, its capture with the subsequent formation of an accretion disk and gravitational energy release. In the case of very massive black holes ($M > 10^8 M_\odot$), the difference between gravitational attractive forces acting on the forward and backward parts of a star is insufficient even on the event horizon for tidal disruption, and the star enters as a whole under the event horizon (in the comoving frame of reference) without producing significant visible effects. The rate of tidal disruption of stars near SMBHs in galactic nuclei is estimated to be one event every 10^4 years per galaxy [124]. As the temperature of the corresponding transient accretion disk at a distance of $3r_{\rm g}$ from the black hole center is $\sim 3 \times 10^5$ K, most of the energy is released in an outburst in the ultraviolet and soft X-ray bands. To date, such transient events due to the tidal disruption of stars have been discovered in a dozen galactic nuclei [124–126]. If a star approaches close enough to the central SMBH event horizon, the form of the outburst is significantly determined by GR effects, which also offers the basic possibility of testing the spacetime metric near the event horizon. Moreover, as the duration of such an outburst is rather long, about one year, the process of tidal disruption of the star in the SMBH gravitational field may be directly observed by high-resolution radio interferometers like Radio-Astron or Millimetron. This also offers the opportunity to test the spacetime metric near the black hole event horizon. Indeed, the star falling onto an SMBH can be treated in the case considered as a test object in the SMBH gravitational field, so its motion and tidal disruption are determined by the spacetime metric of the black hole.

Stars which have avoided total tidal disruption near an SMBH may demonstrate abruptly peculiar properties: rapid axial rotation, strong mixing, intensive mass loss, etc. [127].

Presently, direct observations of a gas cloud approaching the SMBH in our galactic center are underway. The origin of this cloud may be related to a nova eruption in the Milky Way center that occurred in 2000 [128]. The passage of this cloud in the immediate vicinity of the black hole is expected to lead to interesting observational appearances. This cloud was discovered in 2012 [129]. The mass of the G2 cloud is less than three Earth masses, the orbit eccentricity is 0.9664 ± 0.0026, the distance to the central SMBH (SgrA*) at the orbit periastron measures 4400 ± 600 gravitational radii, and the time of the periastron passage falls in the year 2013.69 ± 0.04 [130]. The radio light curve from the G2 cloud passage near the galactic center is presented in paper [131].

Finally, we should mention the possibility of direct proof of the existence of black holes in the Universe by observing gravitational waves from coalescing binary black holes [6, 132]. Observations made with first-generation laser interferometers [133] have not yet discovered gravitational waves incoming from cosmos. However, advanced second-generation laser interferometers will start to operate in a few years with a sensitivity increased by 1–2 orders of magnitude [6, 134]. It is hoped that gravitational wave bursts from coalescing binary black holes will then be detected. Thus far, the gravitational wave signals from coalescing binary black holes (gravitational-wave 'light curves') have been numerically calculated [132, 134] for different black hole parameters. A comparison with forthcoming observations will give the unique chance to study the dynamical characteristics of spacetime during black hole coalescence and, hence, will permit proving the existence of black holes, as well as offering a rigorous test of GR in extremely strong gravitational fields.

7. Conclusion

After forty years of observational studies of black holes, there are almost no doubts that these extreme objects really exist in

the Universe. Therefore, for most of the last two decades most researchers have been using the term 'black hole' instead of the more cautious 'black hole candidate'. This is due to the fact that all observations of these massive and very compact objects are in beautiful agreement with GR predictions for black holes.

Two unexpected results of black hole demography should be emphasized, which need further theoretical studies: the unusual (flat) stellar black hole mass distribution, and the very rapid growth rate of supermassive black holes (the characteristic time is shorter than one billion years).

The launch into orbit of the Russian space interferometer RadioAstron, as well as progress in short-wavelength VLBI observations (the Event Horizon Telescope), now offers the real opportunity to image SMBH shadows in the centers of nearby galaxies and to watch processes near black hole horizons.

This gives us hope that in the nearest future the conclusive proof of the existence of black holes in the Universe will be secured, which will be a breakthrough in our understanding of the concepts of matter and spacetime.

References

1. Zel'dovich Ya B *Sov. Phys. Dokl.* **9** 195 (1964); *Dokl. Akad. Nauk SSSR* **155** 67 (1964)
2. Salpeter E E *Astrophys. J.* **140** 796 (1964)
3. Gillessen S et al. *Astrophys. J.* **692** 1075 (2009)
4. Cherepashchuk A M *Phys. Usp.* **46** 335 (2003); *Usp. Fiz. Nauk* **173** 345 (2003)
5. Novikov I D, Frolov V P *Physics of Black Holes* (Dordrecht: Kluwer Acad., 1989); Translated from Russian: *Fizika Chernykh Dyr* (Moscow: Nauka, 1986) p. 88
6. Novikov I D, Frolov V P *Phys. Usp.* **44** 291 (2001); *Usp. Fiz. Nauk* **171** 307 (2001)
7. Logunov A A *Teoriya Gravitatsionnogo Polya* (Theory of Gravitational Field) (Moscow: Nauka, 2000)
8. Babak S V, Grishchuk L P *Int. J. Mod. Phys.* **12** 1905 (2003)
9. Shakura N I, Sunyaev R A *Astron. Astrophys.* **24** 337 (1973)
10. Pringle J E, Rees M J *Astron. Astrophys.* **21** 1 (1972)
11. Novikov I D, Thorne K S, in *Black Holes* (Eds C DeWitt, B S DeWitt) (New York: Gordon and Breach, 1973) p. 343
12. Remillard R A, McClintock J E *Annu. Rev. Astron. Astrophys.* **44** 49 (2006)
13. McClintock J E, in *Short-Period Binary Stars: Observations, Analyses, and Results* (Eds E F Milone, D A Leahy, D W Hobill) (Berlin: Springer, 2008) p. 3
14. Cherepashchuk A M *Phys. Usp.* **54** 1061 (2011); *Usp. Fiz. Nauk* **181** 1097 (2011)
15. Cherepashchuk A M *Tesnye Dvoinye Zvezdy* (Close Binary Stars) Pt. I (Moscow: Fizmatlit, 2013); *Tesnye Dvoinye Zvezdy* (Close Binary Stars) Pt. II (Moscow: Fizmatlit, 2013)
16. Guseinov O Kh, Zel'dovich Ya B *Sov. Astron.* **10** 251 (1966); *Astron. Zh.* **43** 313 (1966)
17. Cherepashchuk A M et al. *Inform. Bull. Variable Stars* (720) (1972)
18. Bahcall J N, Bahcall N A *Astrophys. J.* **178** L1 (1972)
19. Lyutyi V M, Syunyaev R A, Cherepashchuk A M *Sov. Astron.* **17** 1 (1973); *Astron. Zh.* **50** 3 (1973)
20. Lyutyi V M, Syunyaev R A, Cherepashchuk A M *Sov. Astron.* **18** 684 (1974); *Astron. Zh.* **51** 1150 (1974)
21. Goncharskii A V, Romanov S Yu, Cherepashchuk A M *Konechnoparametricheskie Obratnye Zadachi Astrofiziki* (Inverse Problems with Finite Number of Parameters in Astrophysics) (Moscow: Izd. MGU, 1991) p. 61
22. Bisnovatyi-Kogan G S, Komberg B V *Sov. Astron.* **18** 217 (1974); *Astron. Zh.* **51** 373 (1974)
23. Kiziltan B et al. *Astrophys. J.* **778** 66 (2013); arXiv:1309.6635
24. Alpar M A et al. *Nature* **300** 728 (1982)
25. McClintock J E, Remillard R A, in *Compact Stellar X-ray Sources* (Eds W Lewin, M van der Klis) (Cambridge Astrophysics Series, No. 39) (Cambridge, UK: Cambridge Univ. Press, 2006) p. 157
26. Cherepashchuk A M *Space Sci. Rev.* **93** 473 (2000)
27. Orosz J A et al. *Nature* **449** 872 (2007)
28. Abubekerov M K, Antokhina E A, Bogomazov A I, Cherepashchuk A M *Astron. Rep.* **53** 232 (2009); *Astron. Zh.* **86** 260 (2009)
29. Davis S W, Done C, Blaes O M *Astrophys. J.* **647** 525 (2006)
30. Liu J et al. *Astrophys. J.* **679** L37 (2008)
31. Liu J et al. *Astrophys. J.* **719** L109 (2010), Erratum
32. Gou L et al. *Astrophys. J.* **701** 1076 (2009)
33. Gou L et al. *Astrophys. J.* **742** 85 (2011)
34. Narayan R, McClintock J E *Mon. Not. R. Astron. Soc.* **419** L69 (2012)
35. Blandford R D, Znajek R L *Mon. Not. R. Astron. Soc.* **179** 433 (1977)
36. Zel'dovich Ya B, Novikov I D *Sov. Phys. Dokl.* **9** 834 (1965); *Dokl. Akad. Nauk SSSR* **158** 811 (1964)
37. Kormendy J, Ho L C *Annu. Rev. Astron. Astrophys.* **51** 511 (2013)
38. Moran J M, Greenhill L J, Herrnstein J R *J. Astrophys. Astron.* **20** 165 (1999)
39. Cherepashchuk A M, Lyutyi V M *Astrophys. Lett.* **13** 165 (1973)
40. Antokhin I I, Bochkarev N G *Sov. Astron.* **27** 261 (1983); *Astron. Zh.* **60** 448 (1983)
41. Blandford R D, McKee C F *Astrophys. J.* **225** 419 (1982)
42. Gaskell C M, Sparke L S *Astrophys. J.* **305** 175 (1986)
43. Dibai E A *Sov. Astron.* **28** 123 (1984); *Astron. Zh.* **61** 209 (1984)
44. Zasov A V, Cherepashchuk A M *Astron. Rep.* **57** 797 (2013); *Astron. Zh.* **90** 871 (2013)
45. Shen Y et al. *Astrophys. J.* **680** 169 (2008)
46. Volonteri M, Rees M J *Astrophys. J.* **650** 669 (2006)
47. Kelly B C et al. *Astrophys. J.* **719** 1315 (2010)
48. Natarajan P, Volonteri M *Mon. Not. R. Astron. Soc.* **422** 2051 (2012)
49. Begelman M C, Volonteri M, Rees M J *Mon. Not. R. Astron. Soc.* **370** 289 (2006)
50. Fabian A C et al. *Mon. Not. R. Astron. Soc.* **238** 729 (1989)
51. Laor A *Astrophys. J.* **376** 90 (1991)
52. Miniutti G et al. *Mon. Not. R. Astron. Soc.* **398** 255 (2009)
53. Patrick A R et al. *Mon. Not. R. Astron. Soc.* **411** 2353 (2011)
54. Patrick A R et al. *Mon. Not. R. Astron. Soc.* **416** 2725 (2011)
55. Brenneman L W et al. *Astrophys. J.* **736** 103 (2011)
56. Thorne K S *Astrophys. J.* **191** 507 (1974)
57. Daly R A *Mon. Not. R. Astron. Soc.* **414** 1253 (2011)
58. Blandford R D, Payne D G *Mon. Not. R. Astron. Soc.* **199** 883 (1982)
59. Gnedin Yu N, Silant'ev N A *Astrophys. Space Phys.* **10** 1 (1997)
60. Gnedin Yu N, Silant'ev N A, Shternin P S *Astron. Lett.* **32** 39 (2006); *Pis'ma Astron. Zh.* **32** 42 (2006)
61. Silant'ev N A et al. *Astron. Astrophys.* **507** 171 (2009)
62. Afanasiev V L et al. *Astron. Lett.* **37** 302 (2011); *Pis'ma Astron. Zh.* **37** 333 (2011)
63. Gnedin Yu N et al. *Astron. Rep.* **56** 573 (2012); *Astron. Zh.* **89** 635 (2012)
64. Gnedin Yu N et al. *Phys. Usp.* **56** 709 (2013); *Usp. Fiz. Nauk* **183** 747 (2013)
65. Wilms J et al. *Mon. Not. R. Astron. Soc.* **328** L27 (2001)
66. Doeleman S S et al. *Nature* **455** 78 (2008)
67. Ford H C et al. *Astrophys. J.* **435** L27 (1994)
68. Gebhardt K et al. *Astrophys. J.* **729** 119 (2011)
69. McHardy I M et al. *Nature* **444** 730 (2006)
70. Merloni A, Heinz S, di Matteo T *Mon. Not. R. Astron. Soc.* **345** 1057 (2003)
71. Titarchuk L, Osherovich V *Astrophys. J.* **542** L111 (2000)
72. Abramowicz M A, Kluźniak W *Astron. Astrophys.* **374** L19 (2001)
73. Török G et al. *Astron. Astrophys.* **436** 1 (2005)
74. Kato Y *Publ. Astron. Soc. Jpn.* **56** 931 (2004)
75. Gierliński M et al. *Nature* **455** 369 (2008)
76. Martynov D Ya *Sov. Phys. Usp.* **15** 786 (1973); *Usp. Fiz. Nauk* **108** 701 (1972)
77. Cherepashchuk A M *Astron. Rep.* **45** 120 (2001); *Astron. Zh.* **78** 145 (2001)
78. Cherepashchuk A M *Phys. Usp.* **45** 896 (2002); *Usp. Fiz. Nauk* **172** 959 (2002)
79. Özel F et al. *Astrophys. J.* **725** 1918 (2010)

80. Postnov K A, Cherepashchuk A M *Astron. Rep.* **47** 989 (2003); *Astron. Zh.* **80** 1075 (2003)
81. Randall L, Sundrum R *Phys. Rev. Lett.* **83** 4690 (1999)
82. Hawking S W *Nature* **248** 30 (1974)
83. Long J C, Price J C *Comptes Rendus Physique* **4** 337 (2003)
84. Johannsen T, Psaltis D, McClintock J E *Astrophys. J.* **691** 997 (2009)
85. Postnov K A, Prokhorov M E *Astron. Rep.* **45** 899 (2001); *Astron. Zh.* **78** 1025 (2003)
86. Fryer C L, Kalogera V *Astrophys. J.* **554** 548 (2001)
87. Belczynski K et al. *Astrophys. J.* **757** 91 (2012)
88. Tutukov A V, Cherepashchuk A M *Astron. Rep.* **48** 39 (2004); *Astron. Zh.* **81** 43 (2004)
89. Ghisellini G et al. *Mon. Not. R. Astron. Soc.* **399** L24 (2009)
90. Cherepashchuk A M *Astron. Rep.* **54** 578 (2010); *Astron. Zh.* **87** 634 (2010)
91. Zasov A V, Cherepashchuk A M, Katkov I Yu *Astron. Rep.* **55** 595 (2011); *Astron. Zh.* **88** 648 (2011)
92. McLure R J, Dunlop J S *Mon. Not. R. Astron. Soc.* **331** 795 (2002)
93. Beifiori A et al. *Mon. Not. R. Astron. Soc.* **419** 2497 (2012)
94. Decarli R et al. *Mon. Not. R. Astron. Soc.* **402** 2453 (2010)
95. Ferrarese L et al. *Astrophys. J.* **644** L21 (2006)
96. Wehner E H, Harris W E *Astrophys. J.* **644** L17 (2006)
97. Leigh N, Böker T, Knigge C *Mon. Not. R. Astron. Soc.* **424** 2130 (2012)
98. Satyapal S et al. *Astrophys. J.* **704** 439 (2009)
99. Graham A W, Spitler L R *Mon. Not. R. Astron. Soc.* **397** 2148 (2009)
100. Neumayer N, Walcher C J *Adv. Astron.* **2012** 709038 (2012)
101. Graham A W *Mon. Not. R. Astron. Soc.* **422** 1586 (2012)
102. Ilyin A S, Zybin K P, Gurevich A V *JETP* **98** 1 (2004); *Zh. Eksp. Teor. Fiz.* **125** 5 (2004)
103. Ferrarese L *Astrophys. J.* **578** 90 (2002)
104. Di Matteo T et al. *Astrophys. J.* **593** 56 (2003)
105. Booth C M, Schaye J *Mon. Not. R. Astron. Soc.* **405** L1 (2010)
106. Baes M et al. *Mon. Not. R. Astron. Soc.* **341** L44 (2003)
107. Zasov A V, Petrochenko L N, Cherepashchuk A M *Astron. Rep.* **49** 362 (2005); *Astron. Zh.* **82** 407 (2005)
108. Baes M et al. *Astron. Astrophys.* **467** 991 (2007)
109. Xu B-X, Wu X-B, Zhao H-S *Astrophys. J.* **664** 198 (2007)
110. Fukue J *Publ. Astron. Soc. Jpn.* **55** 155 (2003)
111. Takahashi R *Astrophys. J.* **611** 996 (2004)
112. Zakharov A F et al. *New Astron.* **10** 479 (2005)
113. Beckwith K, Done C *Mon. Not. R. Astron. Soc.* **359** 1217 (2005)
114. Huang L et al. *Mon. Not. R. Astron. Soc.* **379** 833 (2007)
115. Takahashi R, Watarai K *Mon. Not. R. Astron. Soc.* **374** 1515 (2007)
116. Dexter J, McKinney J C, Agol E *Mon. Not. R. Astron. Soc.* **421** 1517 (2012)
117. Blandford R D, in *Lighthouses of the Universe: The Most Luminous Celestial Objects and Their Use for Cosmology: Proc. of the MPA/ESO/MPE/USM Joint Astronomy Conf., Garching, Germany, 6 – 10 August 2001* (Eds M Gilfanov, R Sunyaev, E Churazov) (Berlin: Springer-Verlag, 2002) p. 381
118. Genzel R et al. *Nature* **425** 934 (2003)
119. Watarai K-Y et al. *Publ. Astron. Soc. Jpn.* **57** 513 (2005)
120. Doeleman S S et al. *Science* **338** 355 (2012)
121. Rees M J *Science* **247** 817 (1990)
122. Khokhlov A, Novikov I D, Pethick C J *Astrophys. J.* **418** 181 (1993)
123. Ivanov P B, Novikov I D *Astrophys. J.* **549** 467 (2001)
124. Komossa S, Greiner J *Astron. Astrophys.* **349** L45 (1999)
125. Komossa S, in *Reviews in Modern Astronomy* Vol. 15 (Ed. R E Schielicke) (Berlin: Wiley-VCH, 2002) p. 27
126. Gezari S et al. *Nature* **485** 217 (2012)
127. Alexander T, Livio M *Astrophys. J.* **560** L143 (2001)
128. Meyer F, Meyer-Hofmeister E *Astron. Astrophys.* **546** L2 (2012)
129. Gillessen S et al. *Nature* **481** 51 (2012)
130. Gillessen S et al. *Astrophys. J.* **763** 78 (2013)
131. Sadowski A et al. *Mon. Not. R. Astron. Soc.* **432** 478 (2013)
132. Thorne K, in *Ginzburg Conf. on Physics, May 28 – June 2, 2012, Moscow, Russia. Abstracts* (Moscow: Lebedev Physical Institute, 2012) p. 33
133. Abbott B P et al. (The LIGO Scientific Collab., The Virgo Collab.) *Nature* **460** 990 (2009)
134. Pretorius F *Astrophys. Space Sci. Library* **359** 305 (2009)